

Sudan University of Science and Technology College of Graduate Studies Biomedical Engineering Department

M.Sc. Thesis

Noise Reducing Using Hybrid Technique In Magnetic Resonances Image

تقليل الضونضاء من صور جهاز الرنين المغنطيسى باستخدام طريقة مهجنة

Submitted By: Samah Gaysar Musa

Supervise By:

Dr. Zeinab Adam Mustafa

Abstract:

Several new techniques are developed within the previous couple of years that convalesce results on special filters by take away the noise additional with success whereas protective the sides within the information .Image de-noising plays an important role in satellite communication and signal processing applications. In this research , I suggest an median filter ,NLmeansfilter ,Total Variation (TV) ,Hybrid Median Filtering (hmedian), Speckle Reducing Anisotropic Diffusion Filtering (srad) and Bilateral Filter and adaptive discreet wavelet technique for image de-noising. The noisy image is passed through One level discrete wavelet transform is applied , which is passed through post-processing hybrid median filter to remove noise in high-high coefficients . Finally, The Inverse discrete wavelet transform is applied to reconstruct the image. .

The Image quality is measured to reconstruct image. I have a tendency to take PSNR ,SNR ,RMES and MSE as a potency issue to envision the effectiveness of planned de-noising formula.

المستخلص:

تم تطوير العديد من التقنيات الجديدة في الأعوام القليلة الماضية لأجل تنقية الصور بمرشحات خاصة وذلك لإزالة التشويش مع النجاح في الاحتفاظ بمعلومات الصور. في هذا البحث، تم اختيار تطبيق المرشحات التالية:

NLmeansfilter ,Total Variation (TV) ,Hybrid Median Filtering و(hmedian), Speckle Reducing Anisotropic Diffusion(srad) Filtering . Bilateral . وبعد ذلك استخدام discreet wavelet . وبعد ذلك استخدام تقيية الصورة المشوشة من خلال تطبيق مستوى واحد من تحويل المويجات المنفصلة لي تفكيك الصورة وبعد ذلك يتم تمرير الجزء ذو الترددات العالية من الصورة المفككة على مرشح المنفصلة لإزالة الضجيج. وأخيرا، يتم تطبيق معكوس تحويل المويجات المنفصلة لإعادة بناء صورة .

و تم قياس جودة الصورة للصورة المرشحة . وذلك عن طريق قياس SNR ،PSNR، و EMES و RMES للتأكد من فعالية الطرق المستخدمة لإزالة التشويش .

Acknowledgements:

I would like to express our special appreciation and thanks to our advisor MMr. Zeinb Adam you have been a tremendous mentor for Me . I thank you from the bottom of our heart for encouraging our research and helping me at every point towards the completion of the thesis. We express our gratitude towards department of biomedical engineering for providing the opportunity to present My thesis. A special thanks to My family for being there with me in the time of need. Words cannot express how grateful I to My mother, father for all the sacrifices they have made on My behalf. These are your blessings and prayers that have sustained My this far. Also this thesis would not had been complete without the blessings and bestowed strength, ability from the almighty god.

List of figures:

Figure (5.1) brain–hemispheric transaxial I original
Figure (4.2) the proposed technique50
Figure (4.1) block diagram of methodology49
Figure (3.15) show Original and Soft thresholded signal
Figure (3.14) Original and Hard thresholded signal
Figure (3.13) Rayleigh distribution
Figure (3.12) Uniform noise
Figure (3. 11)The PDF of Salt and Pepper noise39
Figure (3.10) The central pixel value is corrupted by Pepper noise38
Figure (3.9) PDF Gaussian noise
Figure (3.8): Laplacian Filter
Figure (3.7): smoothing filter29
Figure (3.6): Spatial Filtering27
Figure (3.5): Spin is influenced selectively in a sagital slice24
Figure (3.4): Scene from animation found
Figure (3.3): the same situations in two and three dimensions20
Figure (3.2): A magnetization M that process20
Figure (3. 1): The spin of the nuclei

Figure (5.2) brain–hemispheric transaxial II original53
Figure (5.3) brain–hemispheric transaxial III original53
Figure (5.4) brain–hemispheric coronal I original54
Figure (5.5) brain–hemispheric coronal II original54
Figure (5.6) brain–hemispheric transaxial I with hybrid median filer55
Figure (5.7) brain–hemispheric transaxial II with hybrid median filter.55
Figure (5.8) brain–hemispheric transaxial III with hybrid median filter.56
Figure (5.9) brain–hemispheric coronal I with hybrid median filter56
Figure (5.10) brain–hemispheric coronal II with hybrid median filter57
Figure (5.11) brain–hemispheric transaxial I with TV filter57
Figure (5.12) brain–hemispheric transaxial II with TV filter58
Figure (5.13) brain–hemispheric transaxial III with TV filter58
Figure (5.14) brain–hemispheric coronal I with TV filter59
Figure (5.15) brain–hemispheric coronal II with TV filter59
Figure (5.16) brain–hemispheric transaxial I with srad filter60
Figure (5.17) brain–hemispheric transaxial II with srad filter60
Figure (5.18) brain–hemispheric transaxial II I with srad filter61

Figure (5.19) brain–hemispheric coronal I with srad filter61
Figure (5.20) brain–hemispheric coronal II with srad filter62
Figure (5.21) brain–hemispheric transaxial I with Bilaterall filter62
Figure (5.22) brain–hemispheric transaxial II with Bilaterall filter63
Figure (5.23) brain–hemispheric transaxial II I with Bilaterall filter63
Figure (5.24) brain–hemispheric coronal I with Bilaterall filter64
Figure (5.25) brain–hemispheric coronal II with Bilaterall filter64
Figure (5.26) brain–hemispheric transaxial I with NLmeansfilter65
Figure (5.27) brain–hemispheric transaxial II with NLmeansfilter65
Figure (5.28) brain–hemispheric transaxial II I with NLmeansfilter66
Figure (5.29) brain-hemispheric coronal I with NLmeansfilter filter66
Figure (5.30) brain-hemispheric coronal II with NLmeansfilter filter67
Figure (5.31) brain–hemispheric transaxial I hybrid median+ wavelet67
Figure (5.32) brain–hemispheric transaxial II hybrid median+ wavelet68
Figure (5.33) brain–hemispheric transaxial I II hybrid median+wavelet68
Figure (5.34) brain–hemispheric coronal I hybrid median wavelet69
Figure (5.35) brain-hemispheric coronal II hybrid median wavelet69
Figure (5.36) brain–hemispheric transaxial I hybrid median +wavelet70

Figure (5.37) brain-hemispheric transaxial II hybrid median + wavelet.70

Figure (5.38)**brain–hemispheric transaxia III**I hybrid median +wavelet..71

Figure (5.39) brain-hemispheric coronal I hybrid median + wavelet.....71

Figure (5.40) brain-hemispheric coronal II hybrid median + wavelet....72

List of tables:

Table(5.1) the results	of filters75	
Table(5.2) the results	of hybrid median filter after using the wavelet7	7.

Contents:

Contents:	NO.
Abstract	I
المستخلص	II
Acknowledgements	III
List of figures	IV
List of tables	V
Contents	VI
Chapter one Introduction	
1.1 Introduction	2
1.2 statement of problem	3
1. 3Objectives	4
1.4 thesis layout	4
Chapter two literature review	
2.1 review studies	6
2.2imaging enhancement	9
Chapter three Theoretical back ground	
3.1 MRI	11
3.2filters	21
3.3 noise	32
3.4 measures of image quality	39
3.5 wavelet transform	40
Chapter four Methodology	
4.1 Data	44
4.2 hardware and software	44
4.3 Procedures	44
Chapter five Result and discussions	
5.1 Original images without noise	48
5.2 discussions	67
Chapter six Conclusion and Recommendation	

6.1 Conclusion	69
6.2Recommendation	69
References	70

Chapter one Introduction

1.1 Introduction:

Today medical imaging technology provides the clinician with a number of complementary fast, flexible, and precise diagnostic tools such as Xray, Computed Tomography (CT) and Magnetic Resonance Imaging (MRI) images. MRI, CT scan and X-ray are the most methodologies widely used to visualize human anatomy. Medical images often need preprocessing before being subjected to statistical analysis. A common preprocessing step is filtering, study spatial domain and transformed domain filtering techniques to solve the noisy problem. Image de-noising is an vital image processing task i.e. as a process itself as well as a comp--onent in other processes. There are many ways to de-noise an image or a set of data and methods exists. The important property of a good image de-noising model is that it should completely remove noise as far as possible as well as preserve edges. Traditionally, there are two types of models i.e. linear model and non-liner model. Generally, linear models are used. The benefits of linear noise removing models is the speed and the limitations of the linear models is, the models are not able to preserve edges of the images in a efficient manner i.e the edges, which are recog--nized as discontinuities in the image, are smeared out. On the other Hand, Non-linear models can handle edges in a much better way than linear models. [1]

Magnetic resonance imaging (MRI) provides detailed images of living tissues, and is used for both brain and body human studies. Data obtained from MR images is used for detecting tissue deformities such as cancers and injuries .MRI imaging is also used when treating brain tumor, ankle and foot. From these high-resolution images, we can derive detailed anatomical information to examine human brain development and discover abnormalities. MRI consists of T1 weighted, T2 weighted and PD (Proton Density) weighted images. To give proper diagnosis and good results, doctors are provided with the different results of enhanced images. Enhancement is a fundamental task in digital image processing and analysis, aiming to improve the appearance of image in terms of human brightness perception.[2]

Digital image plays an important role in our daily life but, they usually suffer from the poor quality of the image, generally with lack of contrast, presence of artifact, blurring, noise and shading due to improper focusing of camera lens, lighting and other factors. Hence we have to improve the

quality of the image for proper analysis which can be done by image enhancement .Noise is defined as, pixel in the image show different intensity value instead of true value of pixels or noise is an unwanted signal that interferes with original image and degrades the quality of the image. Noise causes the random variations of image intensity and poor visibility of pixel. De-noising is a process of removing noise from the image. Image de-noising is not an easy task because it introduces blurring and artifacts in image. There are different types of de-noising technique and their application depends upon type of noise present in the image. Image de-noising technique classified into two categories. i.e., Spatial domain filtering where pixels are operated directly and Transform domain where transfornations are used to de-noise the image.[3]

1.2 Statement of Problem:

The medical images is the most importance tool for the doctors to diagnostic disease ,and the decision of them dependent on the images . any problem in image like blurring , little of illumination or inappropriate size me be lead to bed image or nosing images . The most problem facing the medical images is the distortion , Especially magnetic reasoning images (MRI). this research is focused on application of digital possessing image tools & filters teachings to enhancement images .

1.3 Objectives:

I propose to review the available literature about enhancement imaging. In this review I will achieve the following two goals:

- 1- To evaluate the potentiality of using filters technique & image possessing tool for enhancement MRI .
- 2- Propose new appropriate technique to selected & enhancement image.

1.4 thesis layout:

the research is document in six chapters:

Chapter one: Introduction

Chapter two: literature review

Chapter three : Theoretical back ground

 ${\bf Chapter\ four}: Methodology$

Chapter five : Result and discussions

Chapter six: Conclusion and Recommendation

Chapter two literature review

2.1 Image Enhancement:

Image enhancement, which is one of the significant techniques in digital image processing, plays an important role in many fields, such as medical image analysis, remote sensing, high definition television, hyper spectral image processing, industrial X-ray image processing, microscopic imaging etc. Image enhancement is a processing on image in order to make it more appropriate for certain applications. [4]

The principal objective of enhancement is to process an image so that the result is more suitable than the original image for a specific application.

[5]

2.2 review studies:

P.Deepa1 and M.Suganthi2 1 proposed [1] :Visual information transmitted in the form of digital image is becoming a major method for communication in modern age but the image obtained after transmission is often corrupted with noise. Removing noise from the original images is still a challenging problem for researchers. There have been several published algorithms and each approach has it assumption, advantages and limitation. This paper presents a review of some significant work in the area of image de-noising filtering techniques applied to medical image. The performance of these techniques investigated the problem of image degradation which might occur during the acquisition of the images, optical effects such as out of focus blurring, camera motion, flatbed scanner and video images. We touch the images of Computed Tomography (CT) with a set of predefined noise levels. The performance of these techniques was evaluated with respect to two quantitative measures, Peak Signal-to-Noise Ratio (PSNR), and Mean Square Error(MSE).[1]

Pratik Vinayak Oak1 proposed [2]: MRI is an advanced medical imaging technique used to produce high quality images of human body and different parts. It gives detail information to analyses the diseases. Medical image processing plays important role to give information in

more extent for such advance images. Original MRI images are generally having low contrast. It is difficult for doctors to analyses them. By increasing the contrast of an image, it will be easy for analyzing because of detailed information. This increase in contrast can be done by number of ways in image processing. This paper compares different methods of enhancement of brain MRI using histogram based techniques.[2]

Sonia Goyal and Seema Baghla proposed [6]: Medical imaging is one of the most important application areas of digital image processing. Processing of various medical images is very much helpful to visualize and extract more details from the image. Many techniques are available for enhancing the quality of medical image. For enhancement of medical images, Contrast Enhancement is one of the most acceptable methods. Different contrast enhancement techniques i.e. Linear Stretch, Histogram Equalization, Region based enhancement, Adaptive enhancement are already available. Choice of Method depends on characteristics of image. This paper deals with contrast enhancement of MRI images and presents here a new approach for contrast enhancement based upon Adaptive Neighborhood technique. A hybrid methodology for enhancement has been presented. Comparative analysis of proposed technique against the existing major contrast enhancement techniques has been performed and results of proposed technique are promising.[6]

Rajulath Banu and Dr. A. Ranjith Ram proposed [7]: In this paper, we study and compare various histogram based Magnetic Resonance Imaging(MRI) enhancement techniques .Image enhancement is a processing on an image in order to make it more appropriate for certain applications. It is used to improve the visual effects and the clarity of image or to make the original image more conducive for computer to process. Contrast enhancement changing the pixels intensity of the input image to utilize maximum possible bins. We need to study and review the different image contrast enhancement techniques because contrast losses the brightness in enhancement of image. By considering this fact, the mixture of global and local contrast enhancement techniques may enhance the contrast of image with preserving its brightness. Generally, MRI images are having low contrast. It may be difficult for analysing because of lack of detailed information. Contrast of MR images can be increased by number of ways in image processing. Histogram based techniques are used to enhance all types of medical images .[7]

Prof. J.Mehena proposed [8] Medical images edge detection is an important work for object recognition of the human organs and it is an important pre-processing step in medical image segmentation and reconstruction. Conventionally, edge is detected according to gradientbased algorithm and template-based algorithm, but they are not so good for noise medical image edge detection. In this paper, basic mathematical morphological theory and operations are introduced, and then a novel mathematical morphological edge detection algorithm is proposed to detect the edge of medical images with salt-and-pepper noise. The simulation results shows that the novel mathematical morphological edge detection algorithm is more efficient for image denoising and edge detection than the usually used template-based edge detection algorithms and general morphological edge detection algorithms. It has been observed that the proposed morphological edge detection algorithm performs better than sobel, prewitt, roberts and canny's edge detection algorithm. In this paper the comparative analysis of various image edge detection techniques is presented using MATLAB 8.0 .[8]

Chapter three Theoretical back ground

3.1 MRI:

Magnetic resonance imaging (MRI) is a spectroscopic imaging technique used in medical settings to produce images of the inside of the human body. MRI is based on the principles of nuclear magnetic resonance (NMR), which is a spectroscopic technique used to obtain microscopic chemical and physical data.[9].

3.1.1 The magnetism of the body:

Equipped with a level of understanding of how magnet needles with and without spin are affected by radio waves, we now turn to the "compass needles" in our very own bodies.[10]

- Most frequently, the MR signal is derived from hydrogen nuclei (meaning the atomic nuclei in the hydrogen atoms). Most of the body's hydrogen is found in the water molecules. Few other nuclei are used for MR. [10]
- Hydrogen nuclei (also called protons) behave as small compass needles that align themselves parallel to the field. This is caused by an intrinsic property called nuclear spin (the nuclei each rotate as shown in figure 3). By the "direction of the nuclear spins" we mean the axis of rotation and hence the direction of the individual "compass needles".[10]
- The compass needles (the spins) are aligned in the field, but due to movements and nuclear interactions in the soup, the alignment only happens partially, very little, actually. There is only a weak tendency for the spins to point along the field. The interactions affect the nuclei more than the field we put on, so the nuclear spins are still largely pointing randomly, even after the patient has been put in the scanner. An analogy: If you leave a bunch of compasses resting, they will all eventually point towards north. However, if you instead put them into a running tumble dryer, they will point in all directions, and the directions of individual compasses will change often, but there will still be a weak tendency for them to point towards north. In the same manner, the nuclei in the body move among each other and often collide, as expressed by the temperature. At body temperature there is only a weak tendency for the nuclei to point towards the scanners north direction. Together, the many

nuclei form a total magnetization (compass needle) called the net magnetization. It is found, in principle, by combining all the many contributions to the magnetization, putting arrows one after another. If an equal number of arrows point in all directions, the net magnetization will thus be zero. Since it is generally the sum of many contributions that swing in synchrony as compass needles, the net magnetization itself swings as a compass needle. It is therefore adequate to keep track of the net magnetization rather than each individual contribution to it. As mentioned above, the nuclei in the body move among each other (thermal motion) and the net magnetization in equilibrium is thus temperature dependent. Interaction between neighboring nuclei obviously happens often in liquids, but they are quite weak due to the small magnetization of the nuclei. Depending on the character and frequency of the interaction, the nuclei precess relatively undisturbed over periods of, for example, 100 ms duration. At any time, there is a certain probability that a nucleus takes part in a dramatic clash with other nuclei, and thus will point in a new direction, but this happens rather infrequently. The net magnetization is equivalent to only around 3 per million nuclear spins oriented along the direction of the field (3 ppm at 1 tesla). This means that the magnetization of a million partially aligned hydrogen nuclei in the scanner equals a total magnetization of only 3 completely aligned nuclei With the gigantic number of hydrogen nuclei (about 1027) found in the body, the net magnetization still becomes measurable. It is proportional to the field: A large field produces a high degree of alignment and thus a large magnetization and better signal-tonoise ratio.[10]

- If the net magnetization has been brought away from equilibrium, so it no longer points along the magnetic field, it will subsequently precess around the field with a frequency of 42 million rotations/second at 1 tesla (42 MHz, megahertz). This is illustrated in figure 4. Eventually it will return to equilibrium (relaxation), but it takes a relatively long time on this timescale (e.g. 100 ms as described above). Meanwhile, radio waves at this frequency are emitted from the body. We measure and analyze those. Notice: The position of the nuclei in the body does not change only their axis of rotation. [10]
- The precession frequency is known as the Larmor frequency in the MR community. The Larmor equation expresses a connection between the

resonance frequency and the magnetic field, and it is said to be the most important equation in MR: $f = \gamma B0$ The equation tells us that the frequency f is proportional to the magnetic field, B0. The proportionality factor is 42 MHz/T for protons. It is called "the gyromagnetic ratio" or simply "gamma". Thus, the resonance frequency for protons in a 1.5 tesla scanner is 63 MHz, for example. The Larmor equation is mainly important for MR since it expresses the possibility of designing techniques based on the frequency differences observed inhomogeneous fields. Examples of such techniques are imaging, motion encoding and spectroscopy .But how is the magnetization rotated away from its starting point? It happens by applying radio waves at the above mentioned frequency. Radio waves are magnetic fields that change direction in time. The powerful stationary field pushes the magnetization so that it processes. Likewise the radio waves push the magnetization around the radio wave field, but since the radio wave field is many thousand times weaker than the static field, the pushes normally amount to nothing. Because of this, we will exploit a resonance phenomenon: By affecting a system rhythmically at an appropriate frequency (the systems resonance frequency), a large effect can be achieved even if the force is relatively weak. A well-known example: Pushing a child sitting on a swing. If we push in synchrony with the swing rhythm, we can achieve considerable effect through a series of rather weak pushes. If, on the other hand, we push against the rhythm (too often or too rarely) we achieve very little, even after many pushes. With radio waves at an appropriate frequency (a resonant radio wave field), we can slowly rotate the magnetization away from equilibrium. "Slowly" here means about one millisecond for a 90 degree turn, which is a relatively long time as the magnetization processes 42 million turns per second at 1 tesla (the magnetization rotates 42 thousand full turns in the time it takes to carry out a 90 degree turn, i.e., quite a lot faster). Figure 6 is a single scene from an animation found at http://www.drcmr.dk/MR that shows how a collection of nuclei each processing around both B0 and a rotating radio wave field as described earlier, together form a net magnetization that likewise moves as described. The strength of the radio waves that are emitted from the body depends on the size of the net magnetization and on the orientation. The greater the oscillations of the net magnetization, the more powerful the emitted radio waves will be. The signal strength is

proportional to the component of the magnetization, that is perpendicular to the magnetic field (the transversal magnetization), while the parallel not contribute (known the longitudinal component does magnetization). In figure 4, the size of the transversal magnetization is the circle radius. If the net magnetization points along the magnetic field (as in equilibrium, to give an example) no measurable radio waves are emitted, even if the nuclei do process individually. This is because the radio wave signals from the individual nuclei are not in phase, meaning that they do not oscillate in synchrony perpendicular to the field. The contributions thereby cancel in accordance with the net magnetization the B0-field being stationary along (there is no transversal magnetization). [10]

• The frequency of the radio waves is in the FM-band so if the door to a scanner room is open, you will see TV and radio communication as artifacts in the images. At lower frequencies we find line frequencies and AM radio. At higher frequencies, we find more TV, mobile phones and (far higher) light, X-ray and gamma radiation. From ultra-violet light and upwards, the radiation becomes "ionizing", meaning that it has sufficient energy to break molecules into pieces. MR scanning uses radio waves very far from such energies. Heating, however, is unavoidable, but does not surpass what the body is used to.[10]

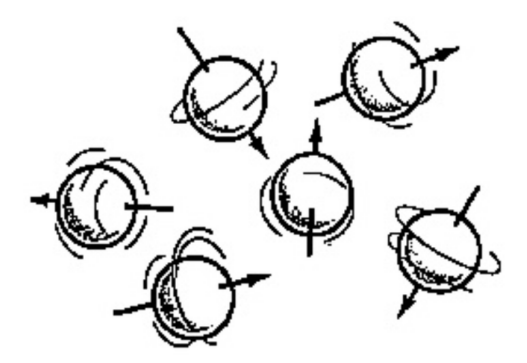


Figure (3. 1): The spin of the nuclei (rotation) makes them magnetic

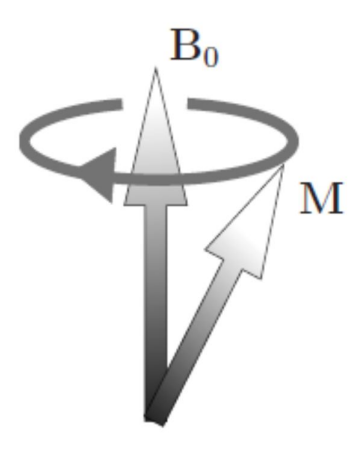


Figure (3.2): A magnetization M that process around the magnetic field B0 because of spin (rotation around M).

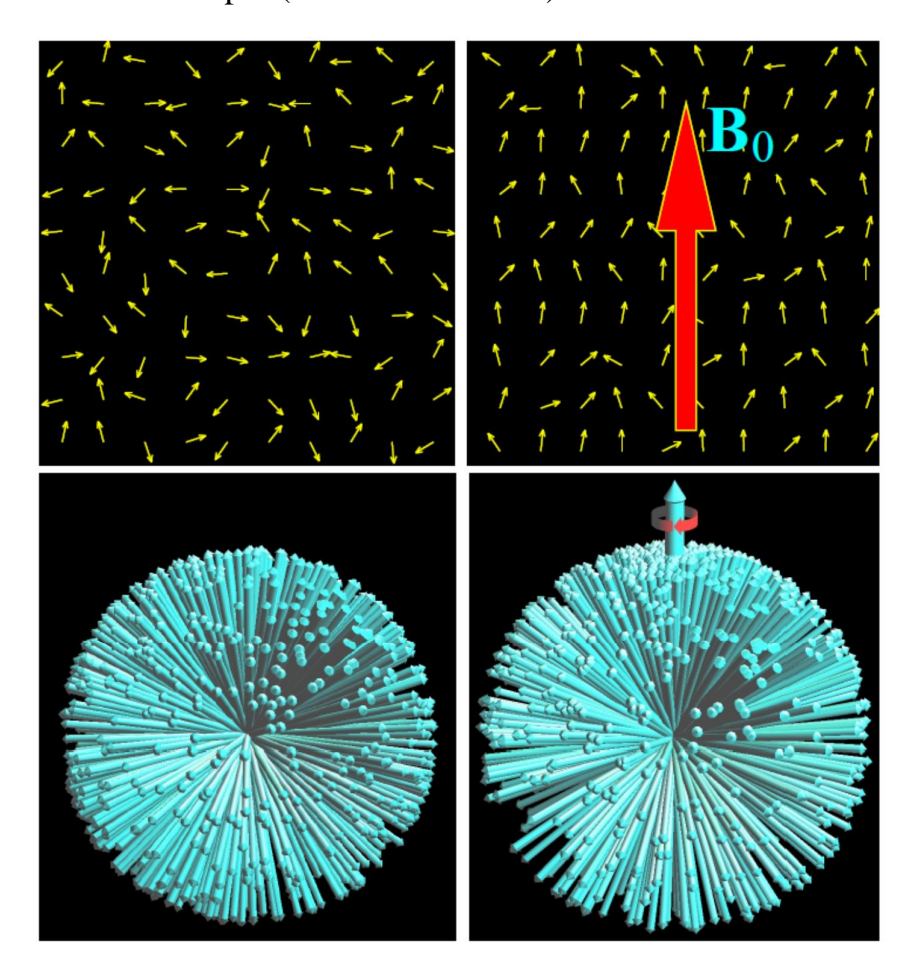


Figure (3.3): The figure shows the same situations in two and three dimensions (top and bottom, respectively).

The nuclear spins are shown as numerous arrows (vectors). In the lower graphs, they are all drawn as beginning in the same point, so that the distribution over directions is clear (implicit coordinate system (Mx,My,Mz)). When a patient arrives in the ward, the situation is as shown in the two graphs to the left: The spins are oriented randomly, with a uniform distribution over directions, meaning that there is about an equal number of spins pointing in all directions. The net magnetization is near zero and the nuclei do not process. When a magnetic field B0 is added, as shown in the two figures to the right, a degree of alignment (order) is established. The field is only shown explicitly in the top right figure, but the effect is visible in both: The direction distribution becomes "skewed" so that a majority of the nuclei point along the field. In the lower right figure, the net magnetization (thick vertical arrow) and the precession (the rotation of the entire ball caused by the magnetic field) are shown. The lower figures appear in the article Is Quantum Mechanics necessary for understanding Magnetic Resonance? Concepts in Magnetic Resonance Part A, 32A (5), 2008.[10]

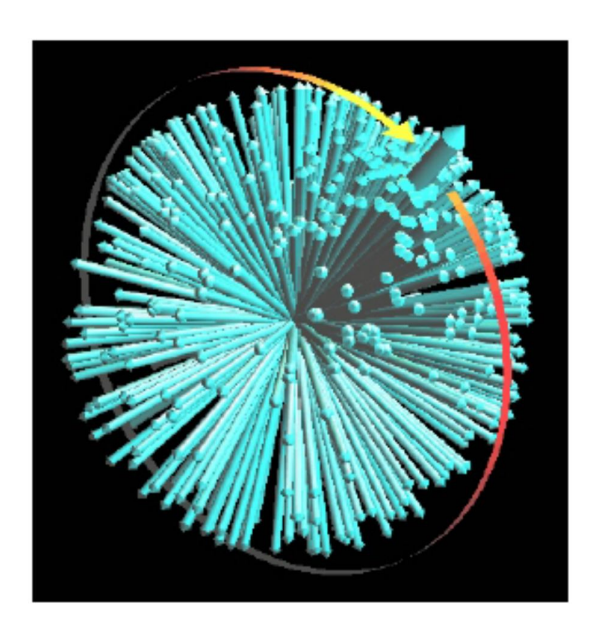


Figure (3.4): Scene from animation found at http://www.drcmr.dk/MR

that shows how radio waves affect a collection of nuclear spins processing around B0 (vertical axis) at the Larmor frequency. The radio wave field that rotates around the same axis at the same frequency, induces simultaneous rotation around a horizontal axis, as symbolized by the circular arrow. The relative orientation of the nuclei does not change,

and it is therefore adequate to realize how the net magnetization (here shown by a thick arrow) is affected by the magnetic field.[10]

3.1.2Weightings:

The contrast in an MR-image is controlled by the choice of measuring method (sequence and sequence parameters, which will be discussed later). For example, we call an image T2-weighted if the acquisition parameters are chosen so the image contrast mainly reflect T2-variations. One must understand, however, that even in a heavily T2-weighted image, the contrast will often reflect more than just T2-variation. To provide an example, variation in water content always results in some contrast. The echo time, TE, is the period from we rotate the magnetization into the transversal plane until we decide to measure the radio waves (a more precise definition will follow later). Meanwhile, a loss of magnetization and signal will occur due to T2-relaxation. The echo time is thus the period within the measurement which gives T2weighting in the images. A long TE compared to T2 will thus result in considerable T2-contrast, but only little signal. The greatest sensitivity to T2-variation will be achieved when TE T2. Often, we will repeat similar measurements several times, e.g. once per line in an image. The repetition -time, TR, is the time between these repetitions. Every time we make such a measurement, we (partially) use the longitudinal magnetization present (the magnetization is rotated into the transversal plane which results in emission of radio waves while the transversal component gradually disappears). If we use the magnetization often (short TR), every repeat will therefore only produce a small signal. If we, on the other hand, wait longer between repetitions (long TR), the magnetization will nearly recover to equilibrium between repetitions. What is meant by short and long TR? It is relative to T1 that is the time scale on which the longitudinal magnetization is rebuilt. If the magnetization is completely rebuilt between measurements for all types of tissue in the scanner, meaning if TR is significantly longer than the maximum T1, the T1contrast will disappear. In this case, the transversal magnetization immediately following the rotation of the nuclei reflects the equilibrium magnetization. The radio waves do so, as well. The equilibrium magnetization is governed by the hydrogen concentration, also known as

the proton density (PD). Thus, we may conclude that using a long TR results in limited T1-weighting but a strong signal. If we apply a shorter TR, the signal is reduced for all types of tissue, but the signal becomes more T1-weighted, meaning that the images will be less intense, but with a relatively greater signal variation between tissues with differing T1. Finally, we can minimize both T1- and T2-contrast, which results in a PD-weighted image. In such an image, variation in the water content is the primary source of contrast, since the proton density is the density of MR-visible hydrogen that is largely proportional to the water content.[10]

3.1.3 imaging:

The most obvious methods for MR imaging could be imagined to be projection or the usage of antennas that can detect where in the body the radio waves are emitted. X-ray and normal microscopy are examples of such "optical" techniques, and it would appear obvious to extend this type of imaging to MR. Optical techniques are, however, "wavelengthlimited", which means that they cannot be used to acquire images more detailed than approximately one wavelength. In other words: Due to fundamental causes, one cannot localize the source of radio waves more precisely than about one wavelength when using lenses or other directionsensitive antennas. The radio waves used in MR scanning are typically several meters long, so with optical techniques we can hardly determine whether the patient is in or outside the scanner (this argument is really only valid in the far field, which is the background for parallel imaging. More on this later). Optical techniques as we know them from binoculars, eyesight, CT, X-ray, ultrasound and microscopes, are thus practically useless for MR-imaging, and a fundamentally different principle is necessary. This principle was introduced by Paul Lauterbur in 1973, and it resulted in the Nobel Prize in Medicine in 2003. Basically, Lauterbur made the protons give their own locations away by making the frequency of the emitted radio waves reflect the position. Lauterbur shared the prize with Sir Peter Mansfield, who also contributed greatly to the development of techniques used in magnetic resonance imaging (MRI).[10]

3.1.4 Principles:

A requirement for MR imaging is that the scanner is equipped with extra electromagnets called "gradient coils" that cause linear field variations.

Direction and strength can be altered as desired. The spatial localization occurs according to different principles, of which the most simple is slice selection. Other forms of coding involve the so-called k-space.[10]

3.1.5 Slice selection:

By using gradient coils, the magnetic field strength can be controlled so that it, for example, increases from left to right ear, while the direction is the same everywhere (along the body). This is called a field gradient from left to right. By making the field inhomogeneous in this way, the resonance frequency varies in the direction of the field gradient. If we then push the protons with radio waves at a certain frequency, the resonance condition will be fulfilled in a plane perpendicular to the gradient as shown in figure 7. The spins in the plane have thus been rotated significantly, while spins in other positions simply vibrate slightly. Thus we have achieved slice selective excitation of the protons and a sagittal slice has been chosen.[10]

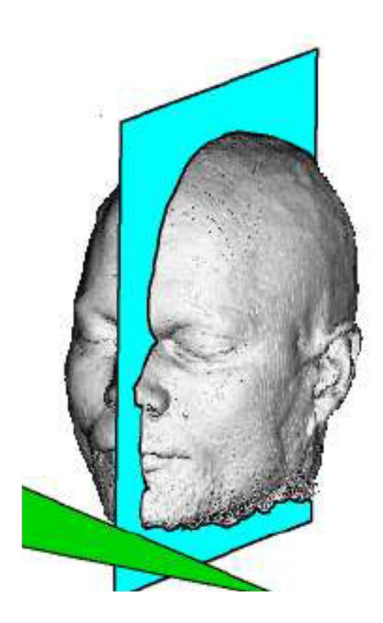


Figure (3.5): Spin is influenced selectively in a sagital slice, if a gradient from left to right is applied while radio waves are transmitted.

3.1.6 Spatial localization within a slice:

After the protons in a slice are excited, they will all emit radio waves. In order to create images of the slice, we must introduce a way to distinguish the signals from different positions within the slice. The fundamental principle can appear a bit foreign, but will be explained in detail at a later

stage. Briefly told, different patterns in the magnetization throughout the slice are created with the help of gradients. The strength of the radio signals that are returned tell us how much the object in the scanner "looks like" the applied pattern. By combining patterns according to their measured similarity to the object, the well-know MR-images are created. What is meant by "patterns" is first illustrated in one dimension, meaning that we consider spins placed on a line (e.g. between the ears) and watch their location and direction immediately after excitation.[10]

As illustrated, immediately after excitation the spins all point in the same direction perpendicular to the magnetic field, which points out of the paper. They will thereafter process around the magnetic field, that is, they will rotate in the plane of the paper at a frequency that is dependent on the magnetic field. Insofar as the field is made to increase from left to right by applying a field gradient briefly, the spins will each turn an angle that depends linearly on the nucleus' position: [10]

the object, the magnetization has rotated several turns. The longer time a gradient is turned on, and the greater the field variation that arises, the more "phase roll" is accumulated (more rotations per unit length). We have through use of gradients, made the spins point in all directions in a controlled fashion and have thus simultaneously lost the signal. This is seen by comparing the two situations above, since the measured magnetization is the sum of all the contributions from the individual spins. When the spins are in phase (that is, pointing in the same direction), they jointly create a considerable magnetization that gives rise to radio waves being emitted. When the spins point in all directions as when a gradient has been applied, their sum is quite small. As a result, comparably weak radio waves are emitted. The gain from using the gradient can thus appear quite small: We have simply lost the signal. That does not, however, have to be the case. Look, for example, at the situation illustrated below where there are not (as above) protons uniformly distributed from left to right, but where there is a regular variation in water content instead.[10]

3.1.7 Image acquisition and echo-time:

the echo time was described as the duration from excitation until the point where radio waves are measured. Since the transversal magnetization in this period is lost on a timescale of T2 (or T * 2, if a refocusing pulse is not used), the echo time TE is thus determining the corresponding relaxation time weighting of the measurement. After the introduction of imaging, we now need to reconsider the definition of echo time, since several positions in k-space are typically being measured after each excitation. A typical approach to imaging is, for example, to measure individual points along a line in k-space one by one after each excitation. The single points (corresponding to different stripe patterns) are consequently not measured at the same time after excitation, and the echo-time definition has therefore become blurry. For echo-planar imaging (EPI), this problem is extreme, since the entire image is measured after a single excitation, meaning that some points in k-space are measured milliseconds after excitation, while others are measured, for example, 100 ms later and thus with a completely different T2 weighting. Is the possibility to characterize T2-weighting by a single parameter therefore lost? No! It turns out that the echo-time definition can be adjusted, so that it still can be interpreted as above. A surprising characteristic comes into play here: Even though parts of k-space are acquired shortly after excitation and other parts a long time after, the reconstructed image looks (contrast-wise) as if it has been acquired at a very certain time after excitation, that being the time where the middle of k-space has been acquired. As such, it makes good sense to define the echo-time as the duration from excitation until the time where the middle of k-space is measured[10]

3.2 filters and noise:

The term spatial domain refers to the image plane itself, and methods in this category are based on direct manipulation of pixels in an image. [5]

As noted in the preceding paragraph, spatial domain techniques operate directly on the pixels of an image. The spatial domain processes are denoted by the expression:[5]

$$g(x,y)=T[f(x,y)]$$
(3.1)

where f(x, y) is the input image, g(x, y) is the output (processed) image, and T is an operator on f defined over a specified neighborhood about point (x, y). In addition, T can operate on a set of images, such as performing the addition of K images for noise reduction.[5]

3.2.1 Spatial Filtering:

This refers to an image operators that change the gray value at any pixel (x,y) depending on the pixel value in a square neighborhood centered at (x,y) using a fixed integer matrix of the same size. The integer matrix is called a filter, mask, kernel or a window. The mechanism of special filtering consists simply of moving the filter mask from pixel to pixel in an image. At each pixel (x,y), the response of the filter at that pixel is calculated using a predefined relationship (linear or nonlinear). The size of mask must be odd (i.e. 3x3, 5x5, e.t.c.) to ensure it has a center. The smallest meaningful size is 3x3. The figure below shows the spatial filter mask .[11]

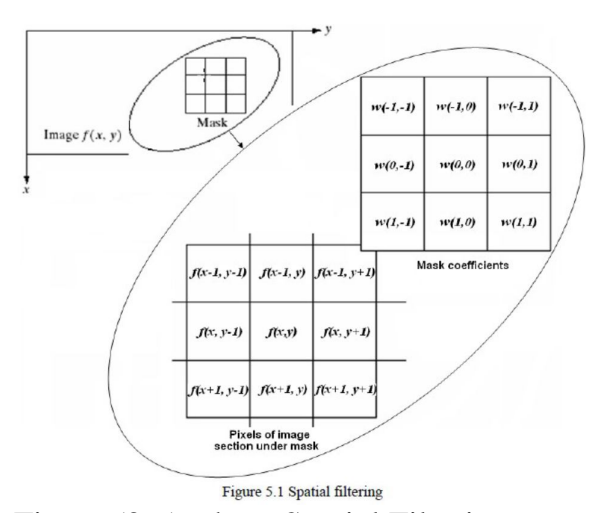


Figure (3.6): show Spatial Filtering

3.2.1.1 Linear Spatial filtering (Convolution):

The process consists of moving the filter mask from pixel to pixel in an image. At each pixel (x,y), the response is given by a sum of products of the filter coefficients and the corresponding image pixels in the area spanned by the filter mask. For the 3x3 mask as shown in figure 3, the result (or response), R of linear filtering [11].

$$R = w(-1,-1)f(x-1,y-1) + w(-1,0)f(x-1,y) + \dots + w(0,0)f(x,y) + \dots + w(1,0)f(x+1,y) + w(1,1)f(x+1,y+1)$$

In general, linear filtering of image f of size MxN with a filter mask of size mxn is given by the expression.

$$g(x, y) = \sum_{s=-a}^{a} \sum_{t=-b}^{b} w(s, t) f(x + s, y + t)$$
(3.2).

Where a = (m-1)/2 and b = (n-1)/2 [8]. To generate a complete filtered image, this equation must be applied for x=0,1,2,....M-1 and y=0,1,...,N-1 [11].

3.2.1.2 Nonlinear Spatial filtering:

The operation also consists of moving the filter mask from pixel to pixel in an image. The filtering operation is based conditionally on the values of the pixels in the neighborhood, and they do not explicitly use coefficients in the sum-of –products manner. For example, noise reduction can be achieved effectively with a nonlinear filter whose basic function is to compute the median gray-level value in the neighborhood in which the filter is located computation of the median is a nonlinear operation.[11]

3.2.2. Smoothing Spatial Filters:

Smoothing filters are used for blurring and noise reduction. Blurring is used preprocessing tasks such as removal of small details from an image prior to (large) object extraction, and bridging of small gaps in lines or curves. Noise reduction can

be accomplished by blurring with a linear filter and also by nonlinear filtering .[2]

3.2.2.1Smoothing Linear Filters:

The output (response) of smoothing, linear filter is simply the average of the pixels contained in the neighborhood of the filter mask. These filters sometimes are called averaging filters. Also, they are also referred to as low-pass filters .Noise and edges consist of sharp transitions in graylevels. Thus smoothing filters are used for noise reduction; however, they have the undesirable side effect that they blur edges. The two figures below shows two 3x3 averaging filters .[11]

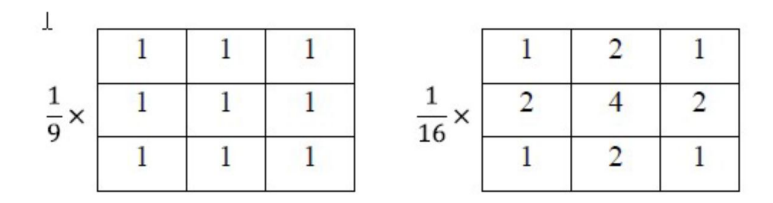


Figure (3.7): show Two 3 x 3 smoothing (averaging) filter masks [11].

The Averaging linear filtering of an image f of size MxN with a filter mask of size mxn is given by the expression [11];

$$\frac{g(x,y) = \sum_{s=-a}^{a} \sum_{t=-b}^{b} w(s,t) f(x+s,y+t)}{\sum_{s=-a}^{a} \sum_{t=-b}^{b} w(s,t)}$$
 (3.3)

To generate a complete filtered image, this equation must be applied for x = 0,1,2,...,M-1 and y=0,1,2,....N-1. The denominator in the above equation is simply the sum of the mask coefficients and, therefore, it is a constant that needs to be computed only once. The following figure below shows an example of applying standard average filter [11].

3.2.3 Order-Statistics (Nonlinear filters):

Order-statistic filters are nonlinear spatial filters whose response is based on ordering (ranking) the pixels contained in the image area encompassed by the filter, and then replacing the value of the center pixel with the value determined by the ranking result. The best known filter in this category is the median filter, which as its name implies, replaces the value of a pixel by the median of the intensity values in the neighborhood of that pixel (the original value of the pixel is included in the computation of the median). Median filters are quite popular because, for certain types of random noise, they provide excellent noise reduction capabilities, with

considerably less blurring than linear smoothing filters of similar size. Median filters are particularly effective in the presence of impulse noise, called salt-and-pepper noise because of its appearance as white and black dots superimposed on an image [11].

3.2.4. Sharpening Spatial Filters:

Sharpening aims to highlight fine details (e.g. edge) in an image, or enhance detail that has been blurred through errors or imperfect capturing devices. Imaging blurring can be achieved using averaging filters, and hence sharpening can be achieved by operators that invert averaging operators[11].

3.2. 4.1 Partial Derivatives of Digital Functions:

The first order partial derivatives of the digital image f(x,y) is

$$\frac{\partial f}{\partial x} = f(x + 1, y) - f(x, y) & \frac{\partial f}{\partial y} = f(x, y + 1) - f(x, y)$$
(3.4)

The first order must be:

- Zero along flat segments (i.e. constant gray values)
- Non-zero at the outset of gray level step or ramp (edges or noise).
- Non-zero along segments of continuing changes i.e. ramps).[11]

The second order partial derivatives of digital images are

$$\frac{\partial 2f}{\partial x^2} = f(x + 1, y) + f(x - 1, y) - 2f(x, y)$$

$$\frac{\partial 2f}{\partial x^2} = f(x, y + 1) + f(x, y - 1) - 2f(x, y)$$
......(3.5)

Second derivative must be;

- Zero along flat segments.
- Non-zero at the outset and of gray-level step or ramp
- Zero along ramps.[11]

3.2.5 Laplacian Filter:

The Laplacian operator of an image f(x,y) is

$$\nabla 2f = \frac{\partial 2f}{\partial x^2} + \frac{\partial 2f}{\partial y^2} \qquad(3.6)$$

The above equation can be implemented using the 3x3 mask as shown below .[14]

$$\begin{bmatrix} -1 & -1 & -1 \\ -1 & 8 & -1 \\ -1 & -1 & -1 \end{bmatrix}$$

Figure (3.8): show Laplacian Filter.

Since the Laplacian filter is a linear spatial filter, we can apply it using the same mechanism of the convolution process. This will produce a Laplacian image that has grayish edge lines and other discontinuities, all superimposed on a dark, featureless background .The figure below shows an example of using Laplacian filter to sharper an image [11].

LINEAR AND NON LINEAR FILTERING TECHNIQUES:

A traditional way to remove noise from image data is to employ spatial filters. Spatial filters can be further classified into linear and non-linear filters. A. Linear Filters

tend to blur sharp edges, destroy lines and other fine image details, and perform poorly in the presence of signal dependent noise.[1]

3.2.6 Mean Filters:

Mean filtering is a simple, intuitive and easy to implement method of smoothing images, i.e. reducing the amount of intensity variation between one pixel and the next. The idea of mean filtering is simply to replace each pixel value in an image with the mean value of its neighbors, including itself. Mean filtering is usually thought of as a convolution filter. Like other convolutions it is based around a kernel, which represents the shape and size of the neighborhood to be sampled when calculating the mean, the mask has a value of N/1, where N is the mask size.[1]

3.2. 7 Gaussian Filters:

The Gaussian smoothing operator is a 2D convolution operator that is used to 'blur' images, remove detail and noise. In this sense it is similar to the mean filter, but it uses a different kernel that represents the shape of a Gaussian. In 2D, the Gaussian distribution follows the equation:

$$\frac{I}{2\pi\sigma} \exp(-\frac{t^2+f^2}{2\sigma^2})$$
(3.7)

Where σ is the standard deviation. The idea of Gaussian Smoothing is to use this 2D distribution as a point-spread Function; achieved by convolution. Once a suitable mask has been calculated, then the Gaussian smoothing can be performed using standard convolution.[1]

3.2.8 Median Filters:

The median filter is normally used to reduce noise in an image, somewhat like the mean filter. However, it often does a better job than the mean filter of preserving useful detail in the image. Median filter considers each pixel in the image in turn and looks at its nearby neighbors to decide whether or not it is representative of its surroundings. Instead of simply replacing the pixel value with the mean of neighboring pixel values; replace it with the median.[1]

3.2.9 2D –Order statistics Filter:

The 2D order-statistic filtering is used to remove the noise and enhance the weak boundaries of medical images. The 2D order-statistic filtering replaces each pixel of an image by the nthorder element in the sorted set of neighbours of size r by specified by the nonzero elements in domain.[1]

3.2.10 Bilateral Filter:

The bilateral filter is a nonlinear, feature preserving image filter, proposed by Smith and Brady and separately by Tomasi and Manduchi . Although, the filter is initially designed to be an alternative to anisotropic diffusion recent researches demonstrate that it has close connections with robust estimation and anisotropic diffusion and the output is a weighted average of the input. They start with standard Gaussian filtering with a spatial kernel f However, the weight of a pixel depends also on a function g in the intensity domain, which decreases the weight of pixels with large intensity differences.[1]

The basic idea underlying bilateral filtering is to do in the range of an image what traditional filters do in its domain. Two pixels can be close to one another, that is, occupy nearby spatial location, or they can be similar to one another, that is, have nearby values, possibly in a perceptually meaningful fashion.

Consider a shift-invariant low-pass domain filter applied to an image:

$$h(x) = k_d^{-1} \int_{\infty}^{\infty} \int_{\infty}^{\infty} f(\epsilon) c(\epsilon - x) d\epsilon \qquad (3.8)$$

The bold font for f and h emphasizes the fact that both input and output images may be multi-band. In order to preserve the DC component, it must be[8]

$$\mathsf{k}_{\mathsf{d}=\int_{\mathsf{m}}^{\infty}\int_{\mathsf{m}}^{\infty}\mathsf{c}(\varepsilon)\mathsf{d}\varepsilon}$$
 (3.9)

3.2.11 Sticks Filter:

After an extensive research, a very strong edge preserving filter known as "sticks". This filter is well known in literature for its capabilities in detection of boundaries and lines in presence of multiplicative noise. In this case, to find the defected region in materials with a high accuracy, it is crucial to conserve all boundaries. To find the lines in the image, it is necessary to determine whether a line passes through each pixel. In sticks filter, a neighbourhood around each pixel is constructed and a search for

lines passing through the center of that neighbourhood is performed. "This is an M-array hypothesis testing, where each of the hypotheses represents a possible line orientation". For simplicity, the neighborhood can be considered to have a square shape. This way, the number of orientations is equal to the number of hypothesis. The set of hypotheses is called "sticks".[1]

3.2.12 Im filter:

Im filter is used to filter a multidimensional array with amultidimensional filter. The result obtained is of same size as the array specified. The parameters specified carry out the multidimensional filtering. The syntax for this is:

A = Imfilter(Y, Z, type1, type2,...)

The values of type1 can be symmetric, replicate, circular, correlate, and type2 can be corr conv etc.[1]

3.2.13 Total Variation (TV):

Total variation based filtering was introduced by Rudin, Osher, and Fatemi .TV de-noising is an effective filtering method for recovering piecewise-constant signals. Many algorithms have been proposed to implement total variation filtering. The one described in these notes is by Chambolle .(Note: Chambolle described another algorithm in).Although the algorithm can be derived in several different ways, the derivation presented here is based on descriptions given in [1, 10]. The derivation is based on the min-max property and the majorization-minimization procedure. Total variation is often used for image filtering and restoration, however, to simplify the presentation of the TV filtering algorithm these notes concentrate on one-dimensional signal filtering only. In addition, the algorithm described here may converge slowly for some problems. Faster algorithms for TV filtering have recently been developed, for example [1, 10]. The development of fast, robust algorithms for TV and related non-linear filtering is an active topic of research.[12]

The total variation (TV) of a signal measures how much the signal changes between signal values. Specifically, the total variation of an N-point signal x(n), $1 \le n \le N$ is defined as[8]:

3.2.14 Linear Despeckle Filter (DsFlsmv):

This filter utilizes the first order statistics, namely the variance and the mean of a pixel neighborhood and may be described with a multiplicative noise model .Hence the algorithms in this class may be traced back to the following equation:

$$f_{i,j} = \overline{g} + k_{i,j}(g_{ij} - \overline{g})$$
(3.11)

Where $f_{i,j}$, is the estimated noise-free pixel value, $g_{i,j}$ is the noisy pixel value in the moving window, g is the local mean value of an N1 \times N2 region surrounding and including pixel $g_{i,j}$, $f_{i,j}$ is a weighting factor, with $k \in [0, 1]$, and g, are

the pixel coordinates. The factor $k_{i,j}$, is a function of the local statistics in a moving window and can be found in the literature [9]as:

$$k_{i,j=(1-\overline{g2}\sigma2)/(\sigma2(1+\sigma_n^2))}$$
 (3.12)

The values σ^2 and σ_n^2 represent the variance in the moving window and the variance of noise in the whole image respectively. The noise variance σ_n^2 , may be calculated for the logarithmically compressed image, by computing the average noise variance over a number of windows with dimensions considerable larger than the filtering window .The moving window size is 5x5 and the number of iterations two.[12]

3.2.15 Hybrid Median Filtering (DsFhmedian):

The filter DsFhmedian ,which is an extension of the median filter, computes the average of the outputs generated by median filtering with three different windows (cross shape window, x-shape window and normal window). Here, a 5x5 size moving window was used with the number of iterations applied to each video frame equal to two.[12]

3.2.16 Speckle Reducing Anisotropic Diffusion Filtering (DsFsrad):

Speckle reducing anisotropic diffusion was proposed in.It is based on setting the conduction coefficient in the diffusion equation using the local frame gradient and the frame Laplacian. The DsFsrad uses two seemingly different methods, namely the Lee and the Frost diffusion filters ,A more general updated function for the output image by extending the partial differential equation versions of the despeckle filter can be found in ;[13]

$$f_{i,j=g_{i,j}} + \frac{1}{ns} \operatorname{div}(c_{srad}(|\nabla_{g}|) \nabla g_{i,j}) \qquad (3.13)$$

$$c2_{srad}(|\nabla g|) = \frac{\frac{1}{2} |\nabla g_{i,j}|^2 - \frac{1}{16} (\nabla 2g_{i,j})^2}{(g_{i,j} + \frac{1}{4} \nabla 2g_{i,j})^2}$$

3.3 Noise:

During image acquisition and transmission, noise is seen in images. This is characterised by noise model. So study of noise model is very important part in image processing. On the other hand, Image de-noising is necessary action in image processing operation. Without the prior knowledge of noise model we cannot elaborate and perform de-noising actions.[14]

Noise tells unwanted information in digital images. Noise produces undesirable effects such as artifacts, unrealistic edges, unseen lines, corners, blurred objects and disturbs background scenes. Digital noise may arise from various kinds of sources such as Charge Coupled Device (CCD) and Complementary Metal Oxide Semiconductor (CMOS) sensors. In some sense, points spreading function (PSF) and modulation transfer function (MTF) have been used for timely, complete and quantitative analysis of noise models. Probability density function (PDF) or Histogram is also used to design and characterize the noise models. [14]

3.3.1 Gaussian Noise Model:

It is also called as electronic noise because it arises in amplifiers or detectors. Gaussian noise caused by natural sources such as thermal vibration of atoms and discrete nature of radiation of warm objects.

Gaussian noise generally disturbs the gray values in digital images. That is why Gaussian noise model essentially designed and characteristics by its PDF or normalizes histogram with respect to gray value.[14]

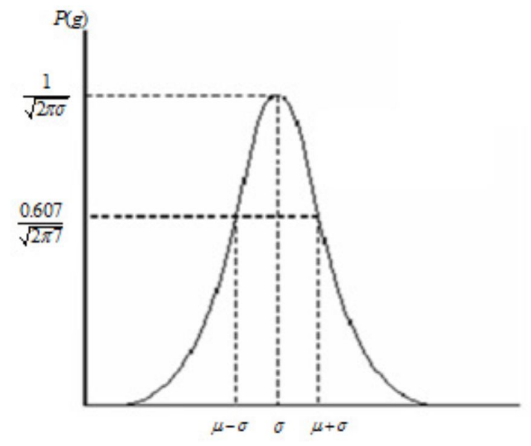


Figure (3.9)show PDF Gaussian noise.

3.3.2 White Noise:

Noise is essentially identified by the noise power. Noise power spectrum is constant in white noise. This noise power is equivalent to power spectral density function. The statement "Gaussian noise is often white noise" is incorrect [14]

However neither Gaussian property implies the white sense. The range of total noise power is $-\infty$ to $+\infty$ available in white noise in frequency domain. That means ideally noise power is infinite in white noise. This fact is fully true because the light emits from the sun has all the frequency components [14].

In white noise, correlation is not possible because of every pixel values are different from their neighbours. That is why autocorrelation is zero.

So that image pixel values are normally disturb positively due to white noise.[14]

3.3.3 Brownian Noise (Fractal Noise):

Colored noise has many names such as Brownian noise or pink noise or flicker noise or 1/f noise. In Brownian noise, power spectral density is proportional to square of frequency over an octave i.e., its power falls on ½ th part (6 dB per octave). Brownian noise caused by Brownian motion. Brownian motion seen due to the random movement of suspended particles in fluid. Brownian noise can also be generated from white noise. However this noise follows non stationary stochastic process. This process follows normal distribution. Statistically fractional Brownian noise is referred to as fractal noise. Fractal noise is caused by natural process. It is different from Gaussian process. [14]

3.3.4 Impulse Valued Noise (Salt and Pepper Noise):

This is also called data drop noise because statistically its drop the original data values. This noise is also referred as salt and pepper noise. However the image is not fully corrupted by salt and pepper noise instead of some pixel values are changed in the image. Although in noisy image, there is a possibilities of some neighbours does not changed. This noise is seen in data transmission. Image pixel values are replaced by corrupted pixel values either maximum 'or' minimum pixel value i.e., 255 'or' 0 respectively, if number of bits are 8 for transmission. Let us consider 3x3 image matrices which are shown in the Fig.(3.10). Suppose the central value of matrices is corrupted by Pepper noise. Therefore, this central value i.e., 212 is given in Fig. (3.10) is replaced by value zero. In this connection, we can say that, this noise is inserted dead pixels either dark or bright. So in a salt and pepper noise, progressively dark pixel values are present in bright region and vice versa.[16]

254	207	210	254	1	207	210
97	212 -	-32	97	-	▶ 0	32
62	106	20	62		106	20

Figure (3.10) The central pixel value is corrupted by Pepper noise.

Inserted dead pixel in the picture is due to errors in analog to digital conversion and errors in bit transmission. The percentagewise estimation of noisy pixels, directly determine from pixel metrics. The PDF of this noise is shown in the Fig. (3.11)

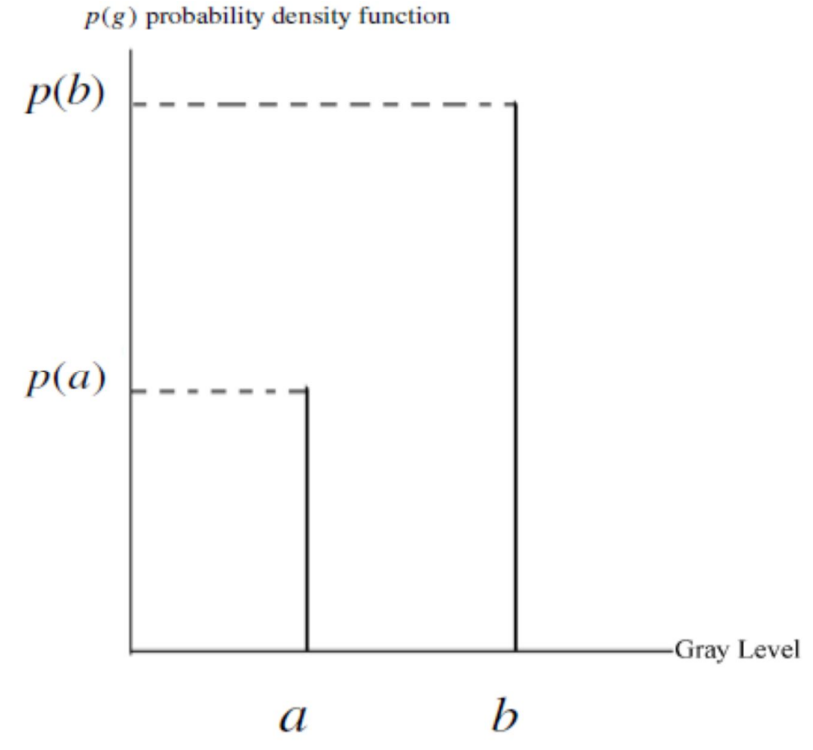


Figure (3. 11) The PDF of Salt and Pepper noise

3.3.5 Periodic Noise:

This noise is generated from electronics interferences, especially in power signal during image acquisition. This noise has special characteristics like spatially dependent and sinusoidal in nature at multiples of specific frequency. It's appears in form of conjugate spots in frequency domain. It can be conveniently removed by using a narrow band reject filter or notch filter.[14]

3.3.6 Quantization noise:

Quantization noise appearance is inherent in amplitude quantization process. It is generally presents due to analog data converted into digital data. In this noise model, the signal to noise ratio (SNR) is limited by minimum and maximum pixel value, P min and P max respectively. Quantization noise obeys the uniform distribution. That is why it is referred as uniform noise. Its PDF is shown in Fig. (3.12).[13]

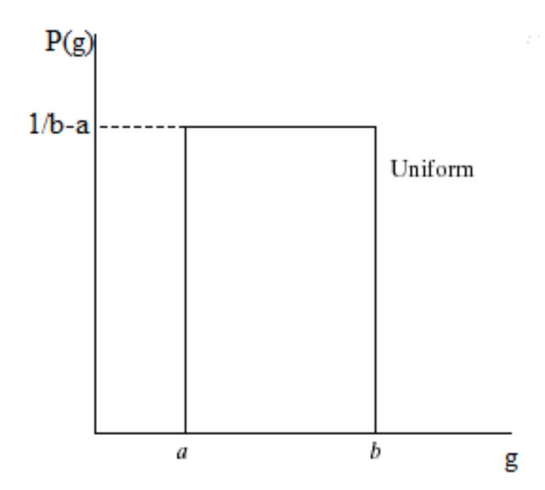


Figure (3.12) show Uniform noise

3.3.7 Speckle Noise:

This noise is multiplicative noise. Their appearance is seen in coherent imaging system such as laser, radar and acoustics etc,. Speckle noise can exist similar in an image as Gaussian noise. Its probability density function follows gamma distribution.[14]

3.3.8 Photon noise (Poisson Noise):

When the physical signal that we observe is based upon light, then the quantum nature of light plays a significant role. A single photon at $\lambda = 500$ nm carries an energy of $E = h \nu = hc/\lambda = 3.97 \times 10$ –19 Joules. Modern CCD cameras are sensitive enough to be able to count individual photons. [15]

3.3.9 Thermal noise:

An additional, stochastic source of electrons in a CCD well is thermal energy. Electrons can be freed from the CCD material itself through thermal vibration and then, trapped in the CCD well, be indistinguishable from "true" photoelectrons. By cooling the CCD chip it is possible to reduce significantly the number of "thermal electrons" that give rise to thermal noise or dark current. As the integration time T increases, the number of thermal electrons increases. The probability distribution of thermal electrons is also a Poisson process where the rate parameter is an increasing function of temperature. There are alternative techniques (to cooling) for suppressing dark current and these usually involve estimating the average dark current for the given integration time and then

subtracting this value from the CCD pixel values before the A/D converter. While this does reduce the dark current average, it does not reduce the dark current standard deviation and it also reduces the possible dynamic range of the signal.[15]

3.3.10 On-chipelectronic noise :

This noise originates in the process of reading the signal from the sensor, in this case through the field effect transistor (FET) of a CCD chip.

3.3.11 Structured Noise:

Structured noise are periodic, stationary or non stationary and aperiodic in nature. If this noise is stationary, it has fixed amplitude, frequency and phase. Structured noise caused by interferences among electronic components. Noise presents in communication channel are in two parts, unstructured noise (u) and structured noise (s). structured noise is also called low rank noise. In a signal processing, it is more advantagable (more realistic) to considering noise model in a lower dimensionality space.[15]

3.3.12 Rayleigh noise:

Rayleigh noise presents in radar range images. In Rayleigh noise, probability density function is given as

$$p(g) = \{\frac{2}{b}(g-a)e^{\frac{-(g-a)^2}{b}} \text{ for } g \ge a \\ 0 \qquad \text{for } < a \qquad \dots (3.14)$$

Where mean u=a+ $\sqrt{\frac{\pi b}{4}}$ and variance $\sigma 2 = \frac{b(4-\pi)}{4}$ are given as ,respectively. [14]

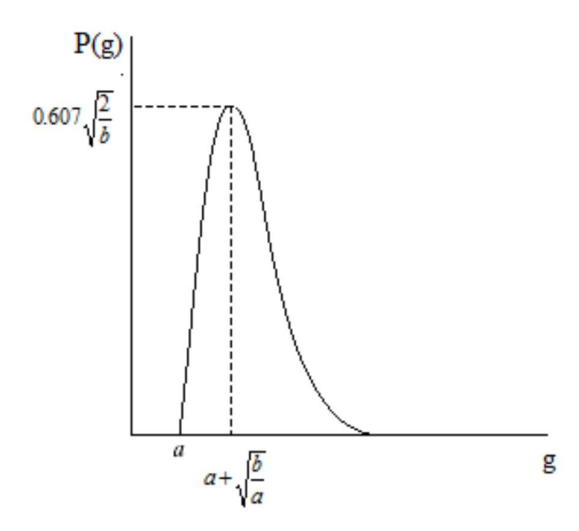


Figure (3.13) Rayleigh distribution.

3.3.13 The Rician Distribution of Noisy MRI Data:

The image intensity in magnetic resonance magnitude images in the presence of noise is shown to be governed by a Rician distribution. Low signal intensities (SNR < 2) are therefore biased due to the noise. It is shown how the underlying noise can be estimated from the images and a simple correction scheme is provided to reduce the bias. The noise characteristics in phase images are also studied and shown to be very different from those of the magnitude images. Common to both, however, is that the noise distributions are nearly Gaussian for SNR larger than two.[16]

It is common practice to assume the noise in magnitude MRI images is described by a Gaussian distribution. The power of the noise is then often estimated from the standard deviation of the pixel signal intensity in an image region with no NMR signal. This can, however, lead to an approximately 60% underestimation of the true noise power. Here we will show that there is a simple analytical relationship between the true noise power and the estimated noise variance. The characteristics of noise in magnitude MRI images has been studied before by Henkelman and the reader is referred to ref. 1 for the formulation of the problem. Henkelman analyzed the problem numerically and did not provide analytical expressions for the noise characteristics. The noise characteristics of quadrature detection, however, have been thoroughly analyzed and documented in applications to communication. During the preparation of this manuscript, we have come across several references in the MRI literature that describe some of the results presented here. Edelstein et al. showed that pure noise in magnitude images is governed by the Rayleigh distribution and later Bernstein et al. provided the closed form solution of the more general Rician distribution in their study on detectability in MRI..[16]

3.4 image quality factors:

The visibility of image quality by human eyes is may be difficult and subjective .so that we tendency to more objective method like SNR, EMSR and PSNR.

3.4.1 EMSR&PSNR:

Comparing restoration results requires a measure of image quality. Two commonly used measures are Mean-Squared Error and Peak Signal-to-Noise Ratio . The mean-squared error (MSE) between two images g(x,y) and $g^{\hat{}}(x,y)$ is:

EMSR =
$$\frac{1}{MN} \sum_{n=1}^{M} \sum_{m=1}^{M} [g^{(n,m)} - g(n,m)]$$
 (3.15)

One problem with mean-squared error is that it depends strongly on the image intensity scaling. A mean-squared error of 100.0 for an 8-bit image (with pixel values in the range 0-255) looks dreadful; but a MSE of 100.0 for a 10-bit image (pixel values in [0,1023]) is barely noticeable. Peak Signal-to-Noise Ratio (PSNR) avoids this problem by scaling the MSE according to the image range:

$$PSNR = -10 \log \frac{EMSR}{S^2} \qquad (3.16)$$

where S is the maximum pixel value. PSNR is measured in decibels (dB). The PSNR measure is also not ideal, but is in common use. Its main failing is that the signal strength is estimated as S^2 , rather than the actual signal strength for the image. PSNR is a good measure for comparing restoration results for the same image, but between-image comparisons of PSNR are meaningless.[17]

4.3.2 Signal-to-Noise ratio:

The signal-to-noise ratio, SNR, can have several definitions. The noise is characterized by its standard deviation, sn. The characterization of the signal can differ. If the signal is known to lie between two boundaries, a min $\le a \le a$ max, then the SNR is defined as[18]:

Bounded signal –
$$SNR = 20\log_{10}(\frac{a_{\max-a_{min}}}{s_n})db$$
 Equation (3.17)

4.3.3 Root Mean Squared Error (MSE):

The root-mean-square deviation (RMSD) or root-mean-square error (RMSE) is a frequently used measure of the differences between values (sample and population values) predicted by a model or an estimator and the values actually observed. The RMSD represents the sample standard deviation of the differences between predicted values and observed values. These individual differences are called residuals when the calculations are performed over the data sample that was used for estimation, and are called prediction errors when computed out-of-sample. The RMSD serves to aggregate the magnitudes of the errors in predictions for various times into a single measure of predictive power. RMSD is a good measure of accuracy, but only to compare forecasting errors of different models for a particular variable and not between variables, as it is scale-dependent.[19]

3.5 wavelet transform:

In most of the applications of image processing, it is essential to analyse a digital signal. If the data will be transformed into any other domain then the structure and features of the signal may be better understood. There are several transforms available like Fourier transform, Hilbert transform, Wavelet transform, etc. The wavelet transform is better than fourier transform because it gives frequency representation of raw signal at any given interval of time, but fourier transform gives only the frequency-amplitude representation of the raw signal, but the time information is lost. So we cannot use the Fourier transform where we need time as well as frequency information at the same time.[20]

3.5.1 Haar wavelet:

Haar wavelet is one of the oldest and simplest type of wavelet. The Haar Transform provides prototype for all other wavelet transforms. Like other wavelet transforms, the Haar Transform decomposes the discrete signal into two sub-signals of half its length. One sub-signal is a running average or trend and other sub-signal is running difference or fluctuation. The advantage of Haar wavelet is that it is fast, memory efficient and conceptually simple.[20]

Thresholding:

Thresholding is the simplest method of image denoising. In this from a gray scale image, thresholding can be used to create binary image. Thresholding is used to segment an image by setting all pixels whose intensity values are above a threshold to a foreground value and all the remaining pixels to a background value. Thresholding is mainly divided into two categories:[20]

3.5.1.1 Hard Thresholding:

Hard threshold is a "keep or kill" procedure and is more intuitively appealing. The transfer function of the Hard thresholding is shown in the figure (3.8). Hard thresholding may seem to be natural. Sometimes pure noise coefficients may pass the hard threshold and this thresholding method is mainly used in medical image processing. [20]

Hard thresholding can be defined as follow:

 $D(U,\lambda)=U$ for all $|D|>\lambda$, 0 otherwiseEquation (3.18)

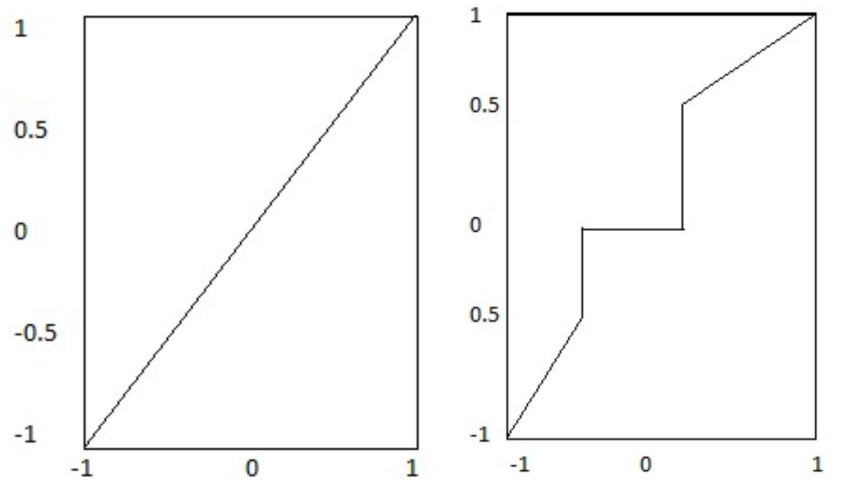


Figure (3.14) show Original (I) and Hard thresholded signal(II)

3.5.1.2 Soft Thresholding:

Soft threshold shrinks coefficients above the threshold in absolute value. The false structures in hard thresholding can be overcomed by soft thresholding. Now a days, wavelet based de-noising methods have received a greater attention. Important features are characterized by large wavelet coefficient across scales in most of the timer scales.[20]

Soft thresholding can be defined as follow:

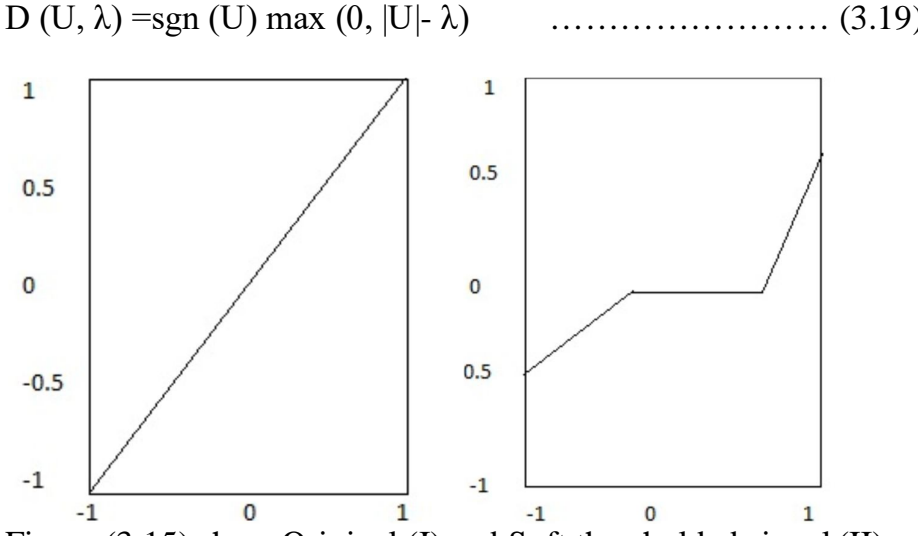


Figure (3.15) show Original (I) and Soft thresholded signal (II)

3.5.2 Daubechies Wavelet Db3:

Daubechies wavelet is the first wavelet family which has set of scaling function which are orthogonal. This wavelet has finite vanishing moments. Daubechies wavelets have balanced frequency responses but nonlinear phase responses. Daubechies wavelets are useful in compression and noise removal of audio signal processing because of its property of overlapping windows and the high frequency coefficient spectrum reflect all high frequency changes. [20]

Chapter four Methodology This study object to enhancement MRI from noise . this doing by use filters and wavelet technique .

Data:

The test data used in this study was acquisition from internet from (http://www.harvarduniversity.com) include normal images.

hardware and software:

A pc hp(530) was the primary hardware piece used in this test. -

Matlab is main software package used in this test .-

Procedures:

The test carried out in this study consist of three steps .step one concern with apply the filters on the images and get result, step two get the calibration indicators (signal to noise ratio 'SNR', peak noise signal ratio 'PNSR', 'RMES', 'MES'), finally apply wavelet in the best filter's result and get the ratio again. That is explained in figures (4.1),(4.2).

Step one:

apply the filters: From previous studies has been assumed using this filters, hybrid median, median2, SRAD, tvdenoise, bilaterall, NLmeansfilter and get results on figures blow.

Step two:

Get SNR,PSNR, RMES ,MES on for each filtered images and results on table one blow .

Finally:

From result of SNR,PSNR, RMES, MES I choosing hybrid median filter to apply the wavelet before using it and apply it in high-high sub-band and low-low sub-band and get the result after filtering in tables one and two and figures blow.

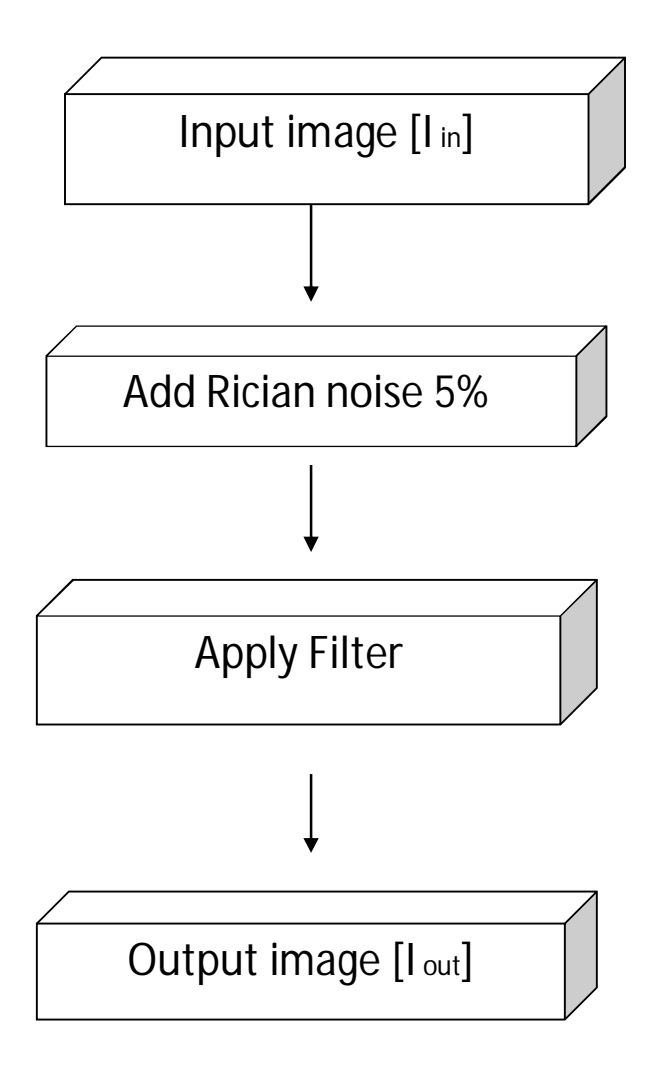


Figure (4.1) show the input image was noise free image the rician noise added to it then de-noised by different types of filters.

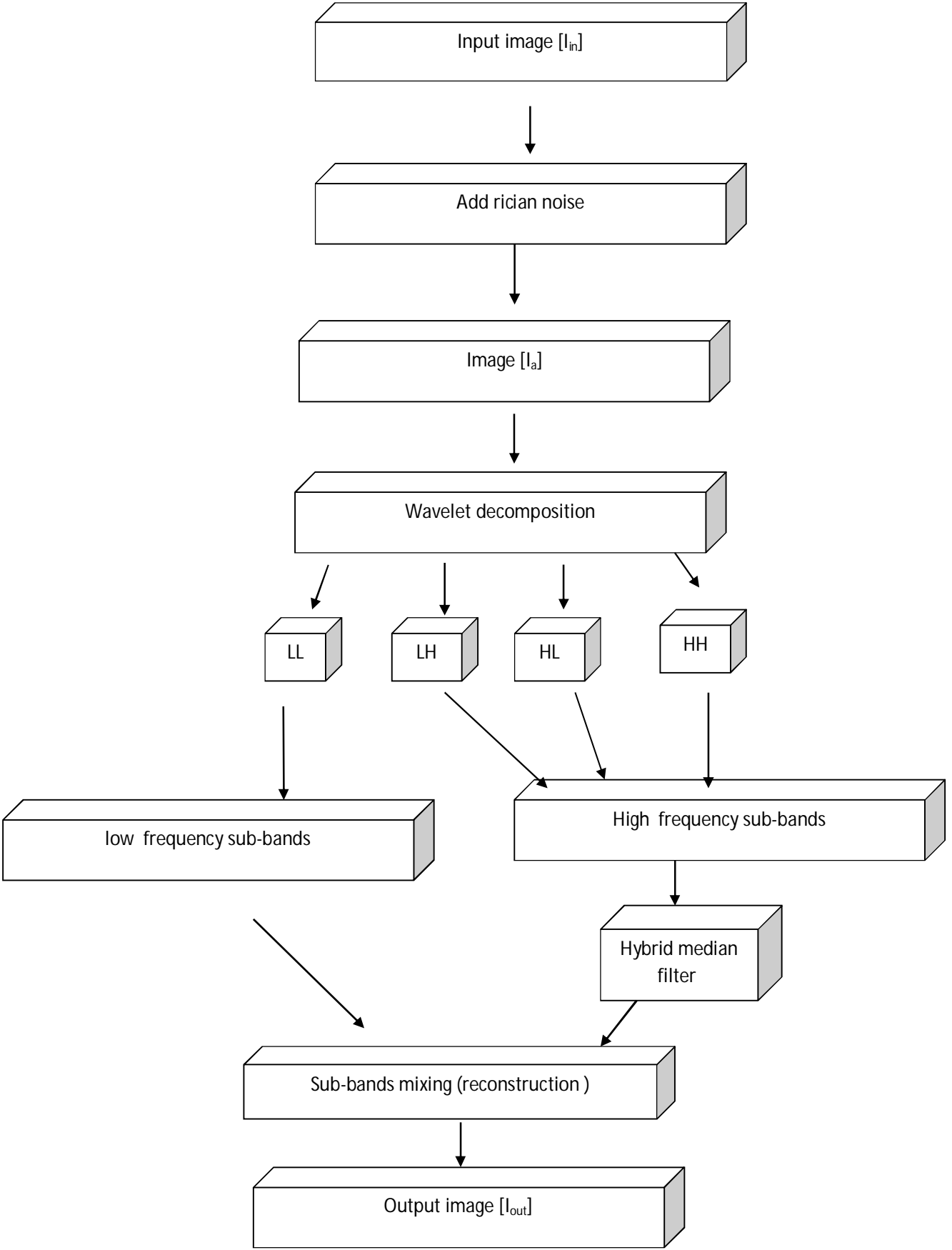


Figure (4.2) show the proposed technique (decomposition wavelet following by hybrid median and reconstructed image).

Chapter five Results & discussions

5.1 Results:

As stated before main object of this study is evaluate the potentiality using filters and wavelet for enhancement MRI with Rician noise. To achieve this objective through apply multi filters and choosing the filter with best result and apply wavelet on the images and filtered, resulted image are recalibration with original image.

5.1.2 Original images without noise:

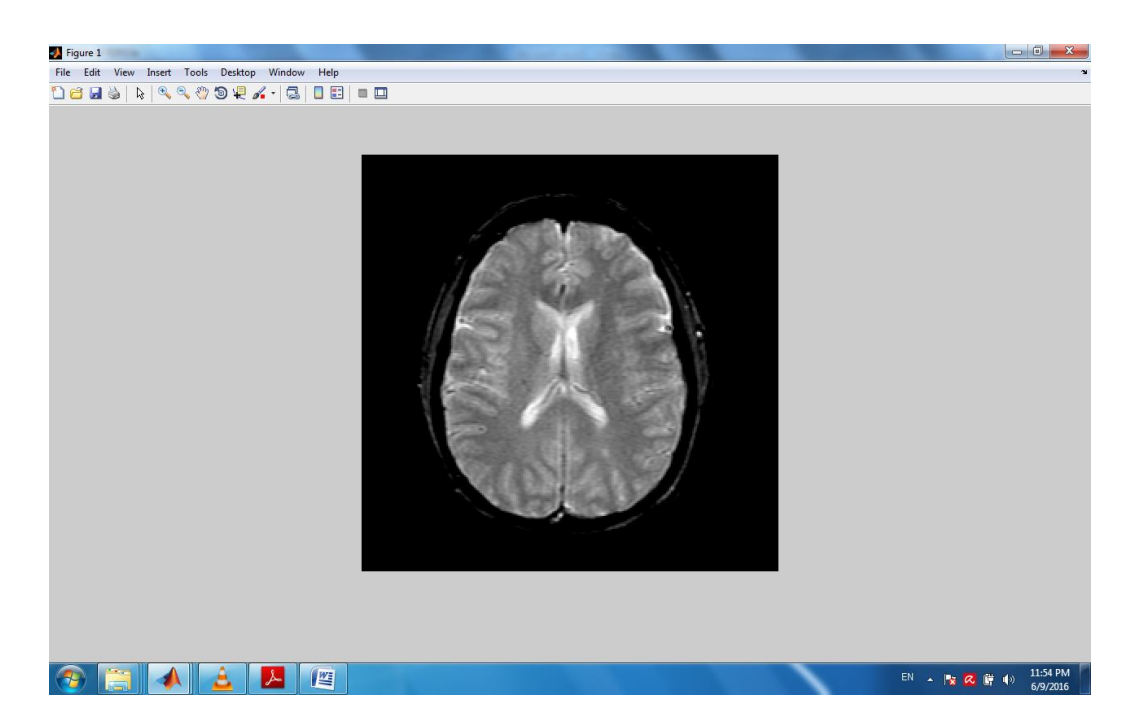


Figure (5.1) show brain-hemispheric transaxial I original

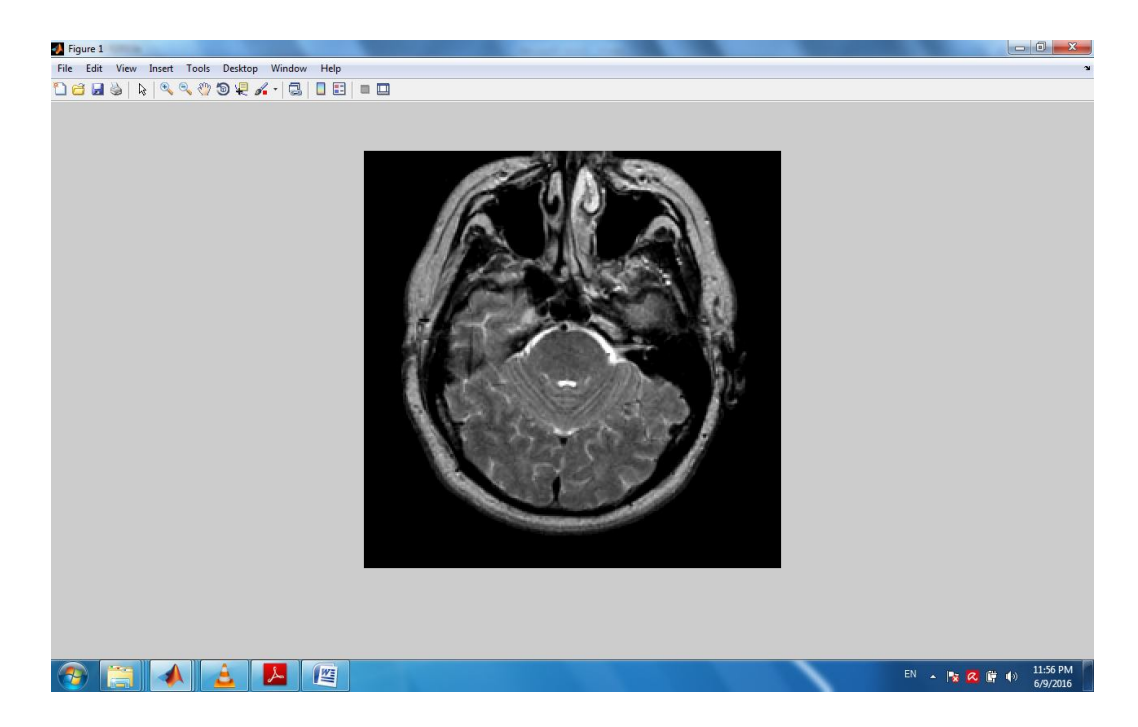


Figure (5.2) show brain-hemispheric transaxial II original

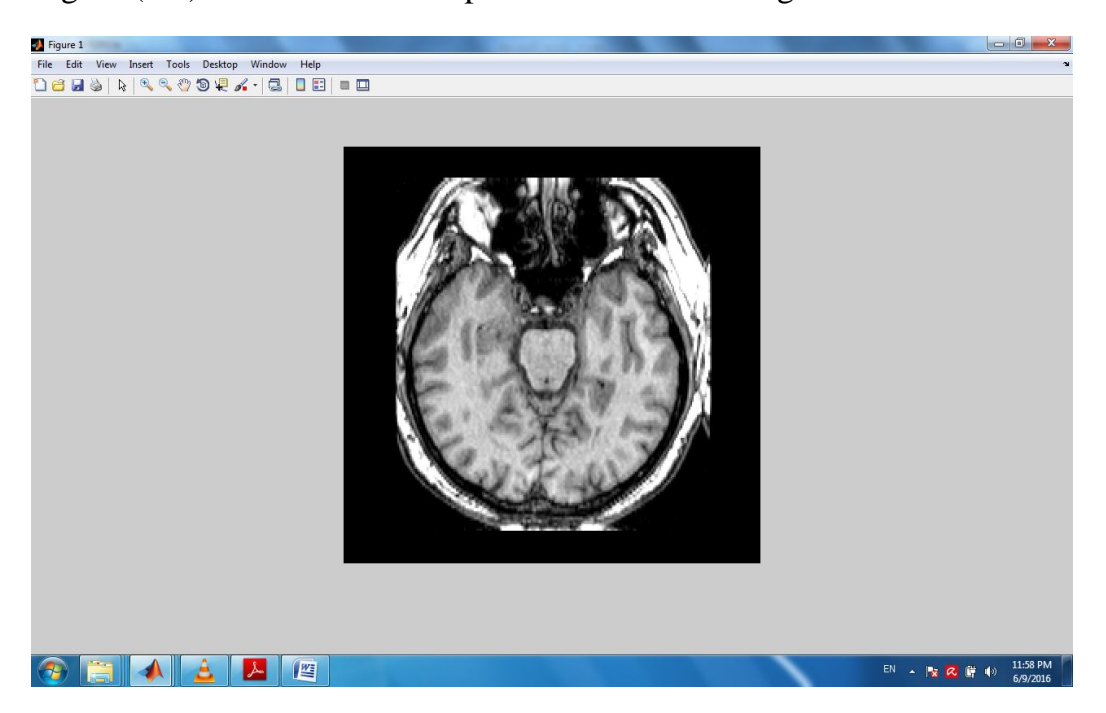


Figure (5.3) show brain-hemispheric transaxial III original

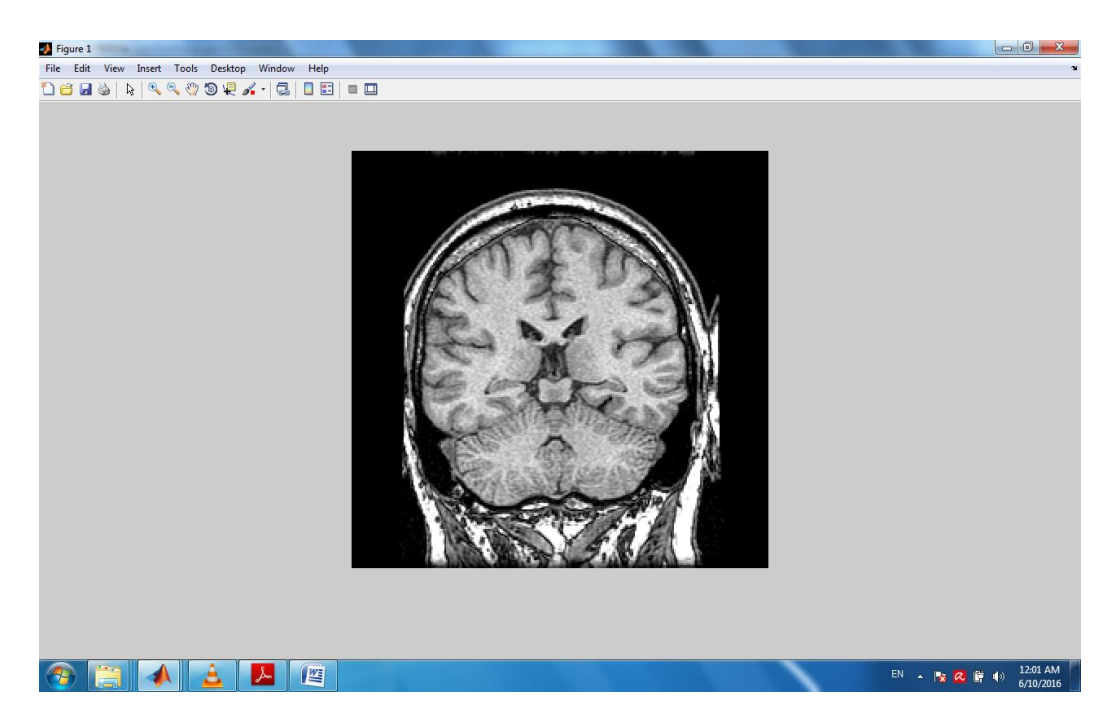


Figure (5.4) show brain-hemispheric coronal II original

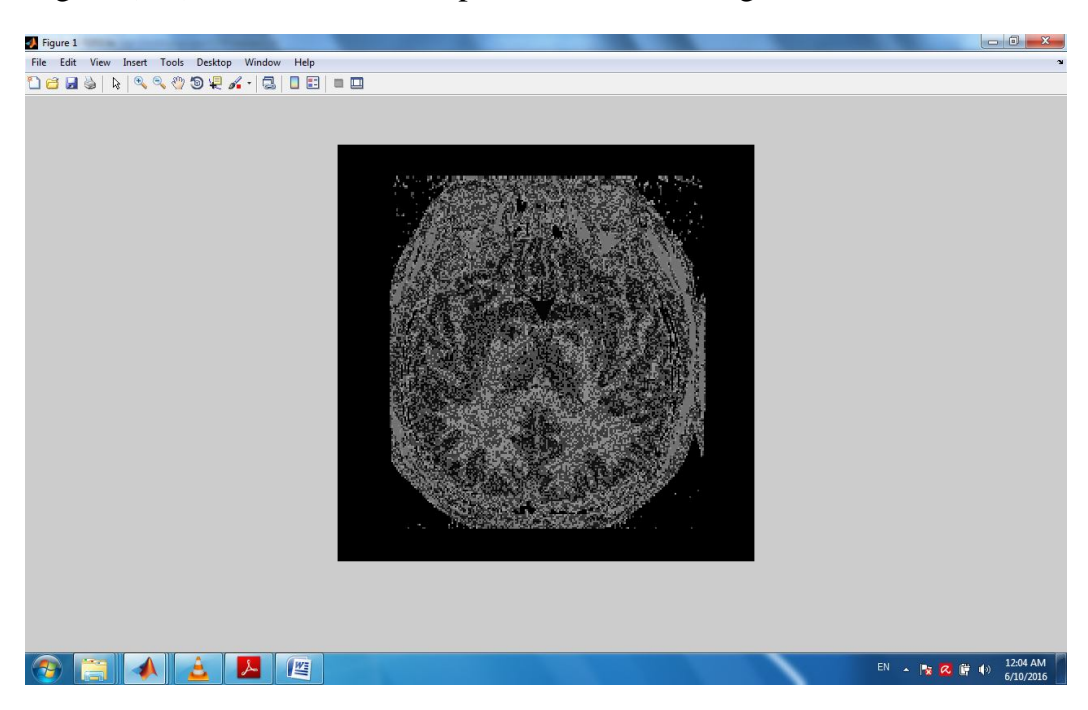


Figure (5.5) show brain-hemispheric coronal II original

5.1.2 Filtered images:

5.1.2.1 hybrid median filters:

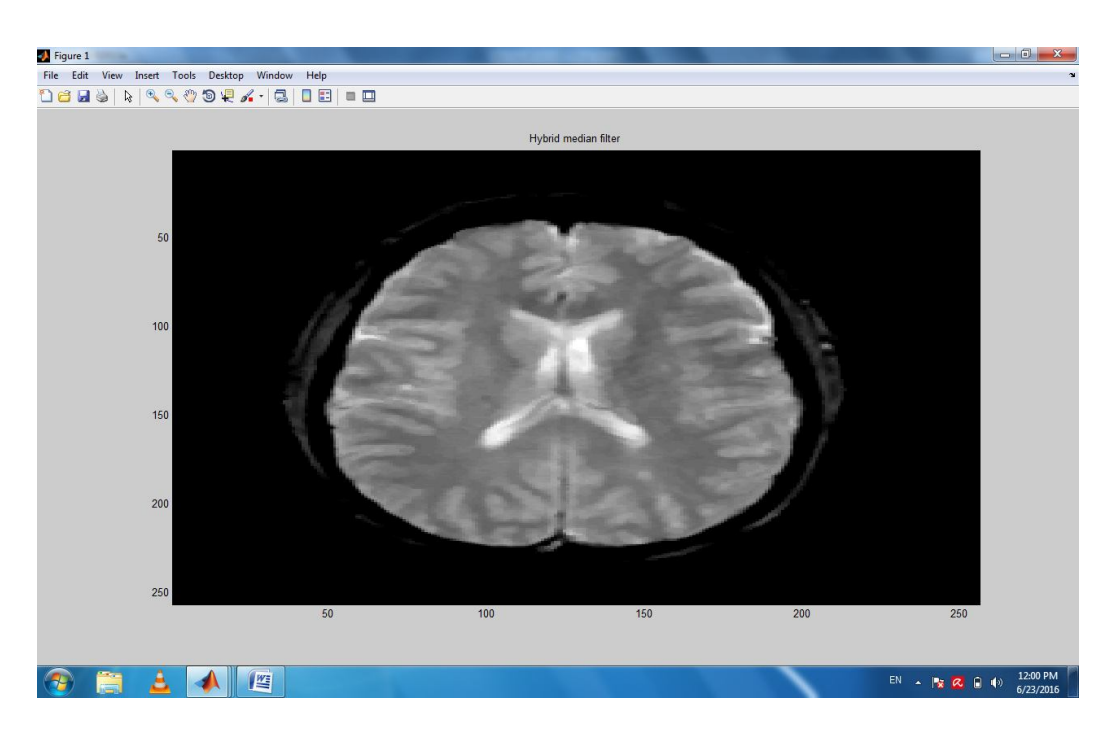


Figure (5.6) brain-hemispheric transaxial I with hybrid median filter

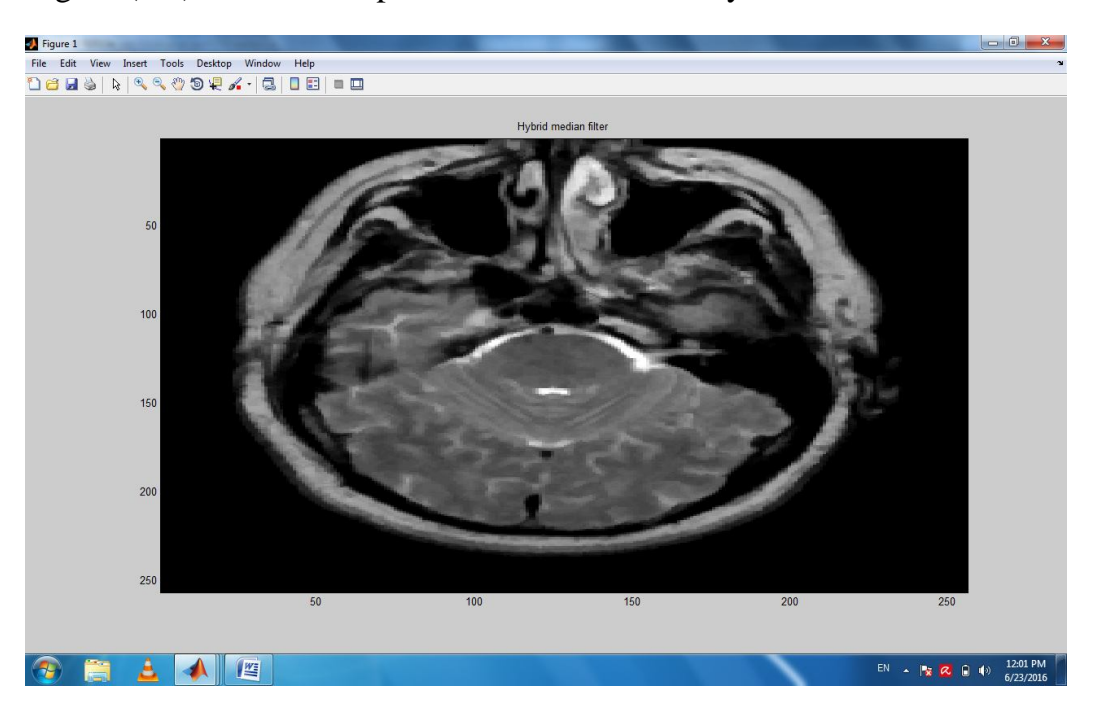


Figure (5.7) brain-hemispheric transaxial II with hybrid median filter

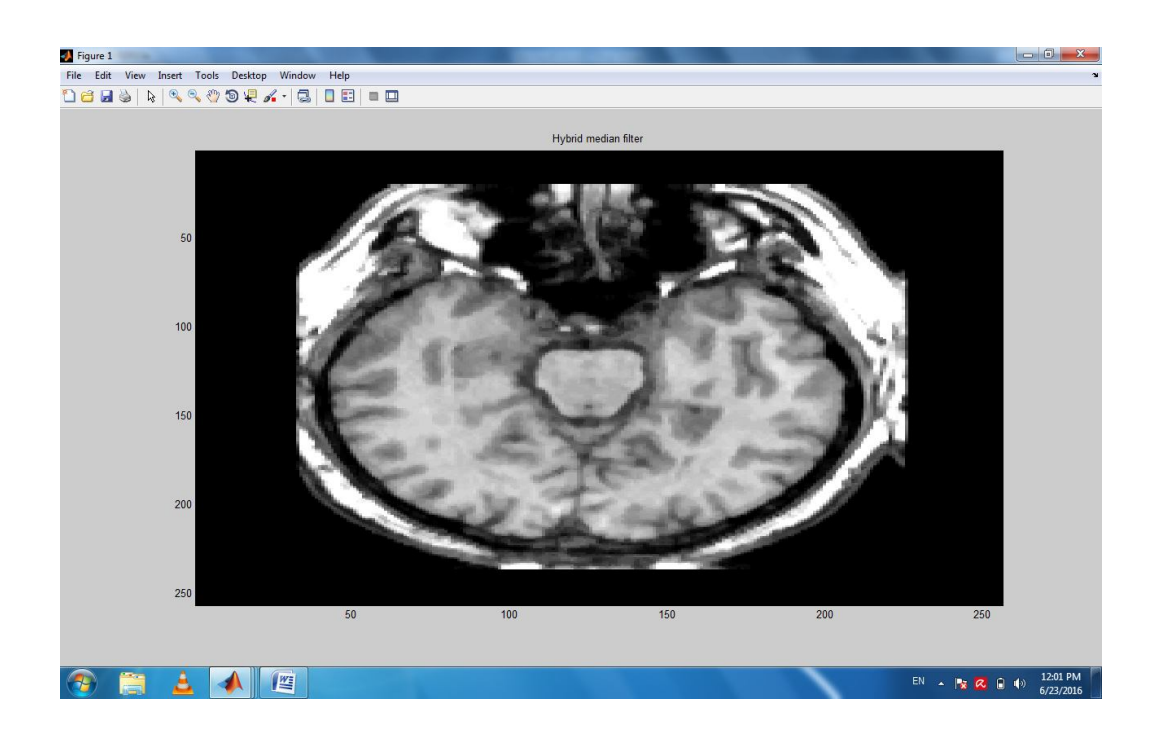


Figure (5.8) show brain–hemispheric transaxial III with hybrid median filter

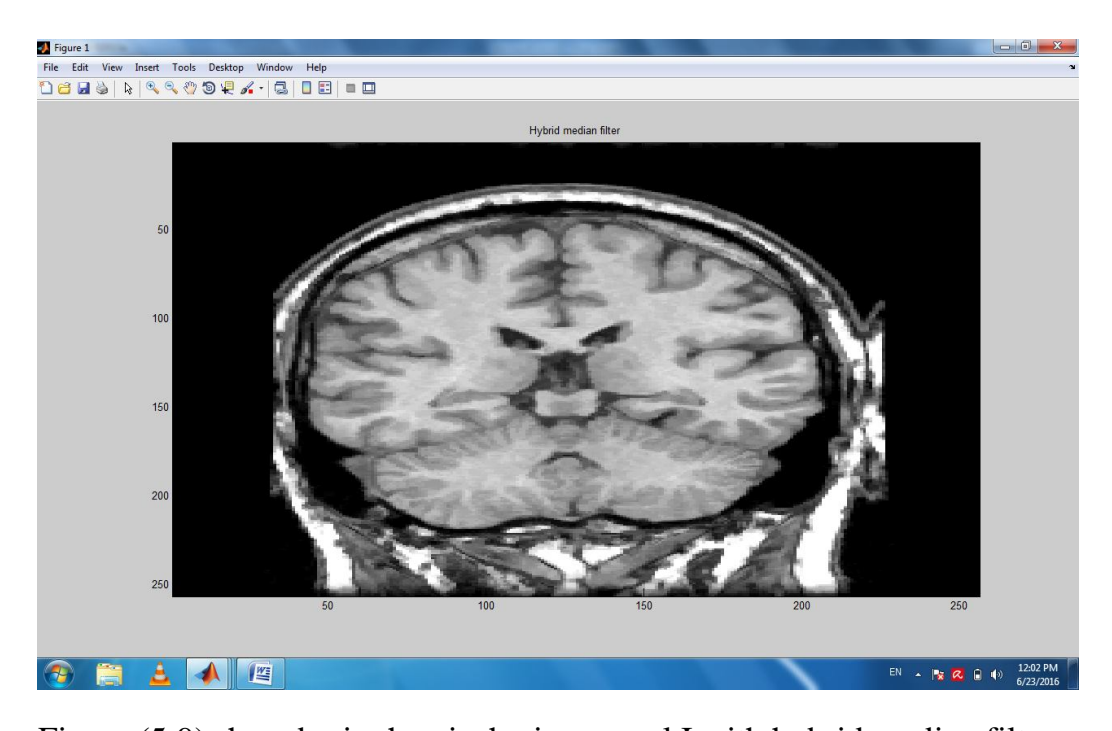


Figure (5.9) show brain-hemispheric coronal I with hybrid median filter

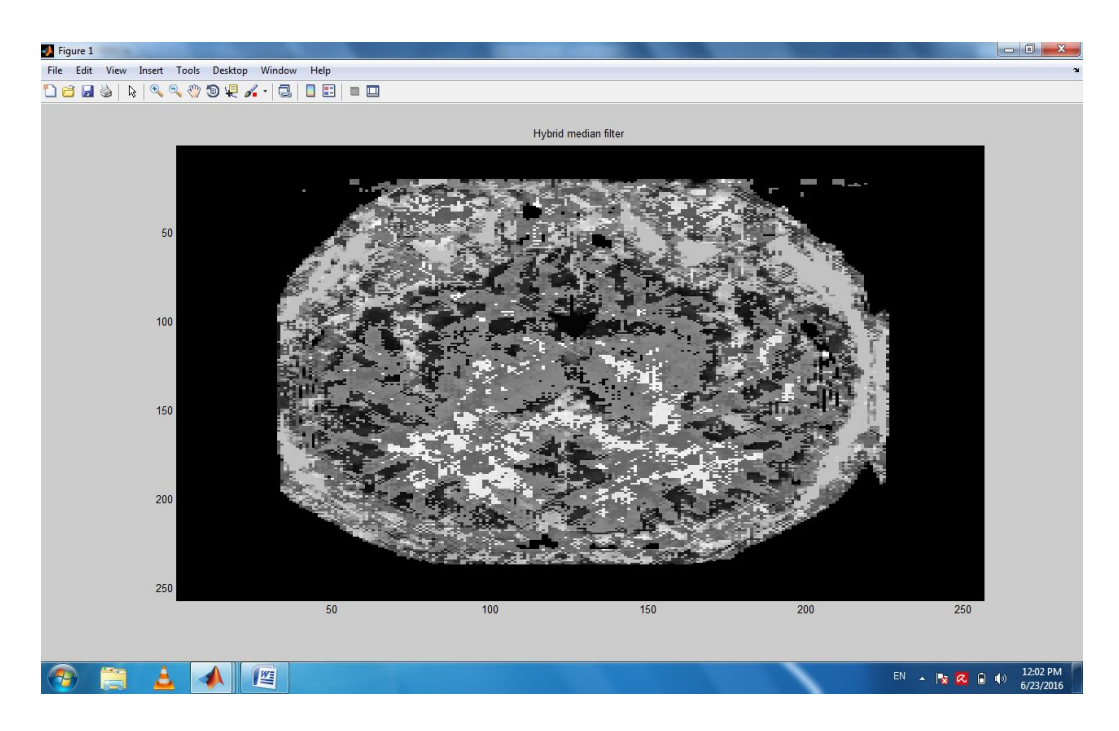


Figure (5.10) show brain–hemispheric coronal II with hybrid median filter

5.1.2.2 Tvdenoise:

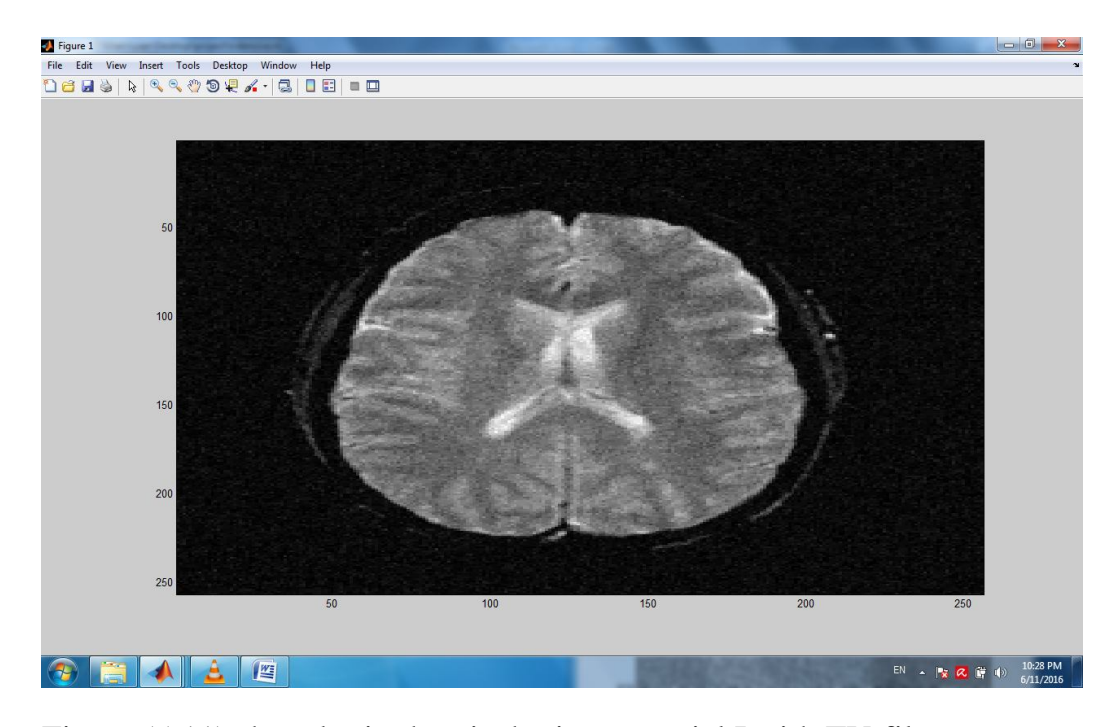


Figure (5.11) show brain-hemispheric transaxial I with TV filter

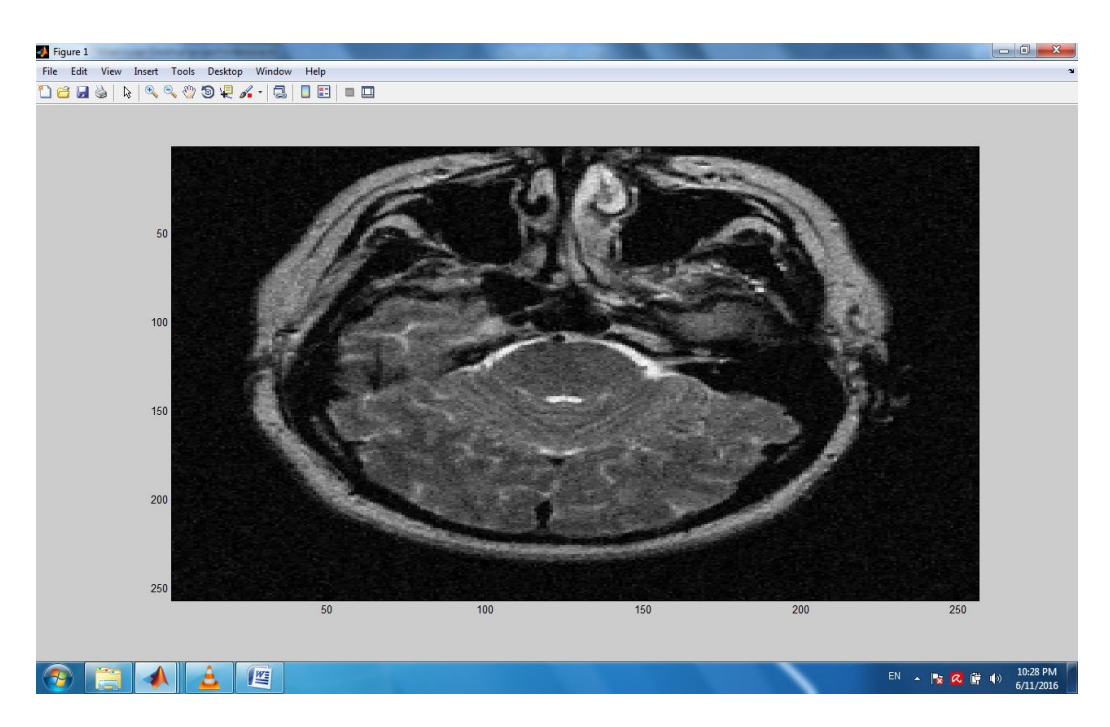


Figure (5.12) show brain-hemispheric transaxial II with TV filter

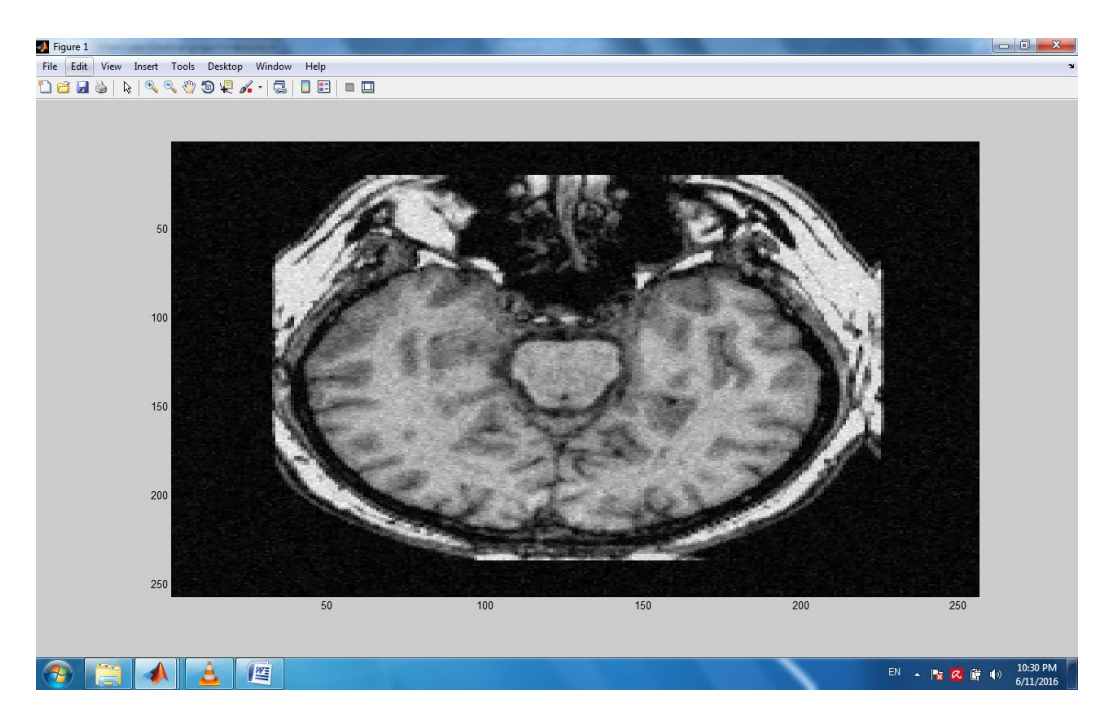


Figure (5.13) show brain-hemispheric transaxial III TV filter



Figure (5.14) show brain-hemispheric coronal I with TV filter

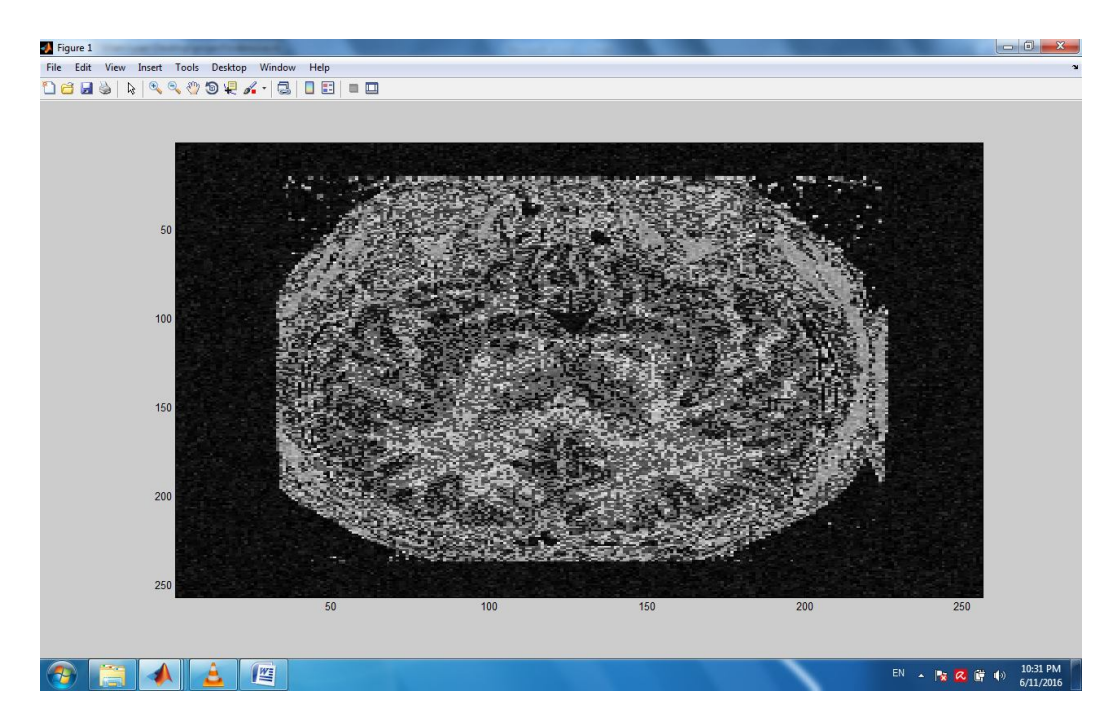


Figure (5.15) show brain-hemispheric coronal II with TV filter

5.1.2.3 srad:

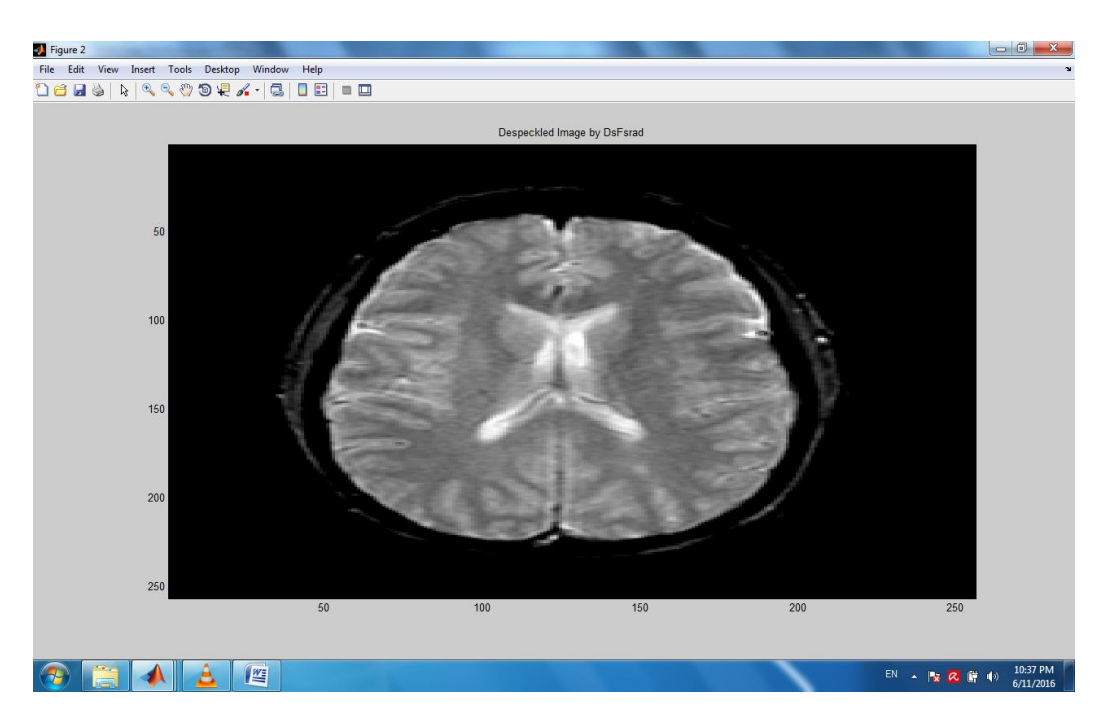


Figure (5.16) brain-hemispheric transaxial I with srad filter

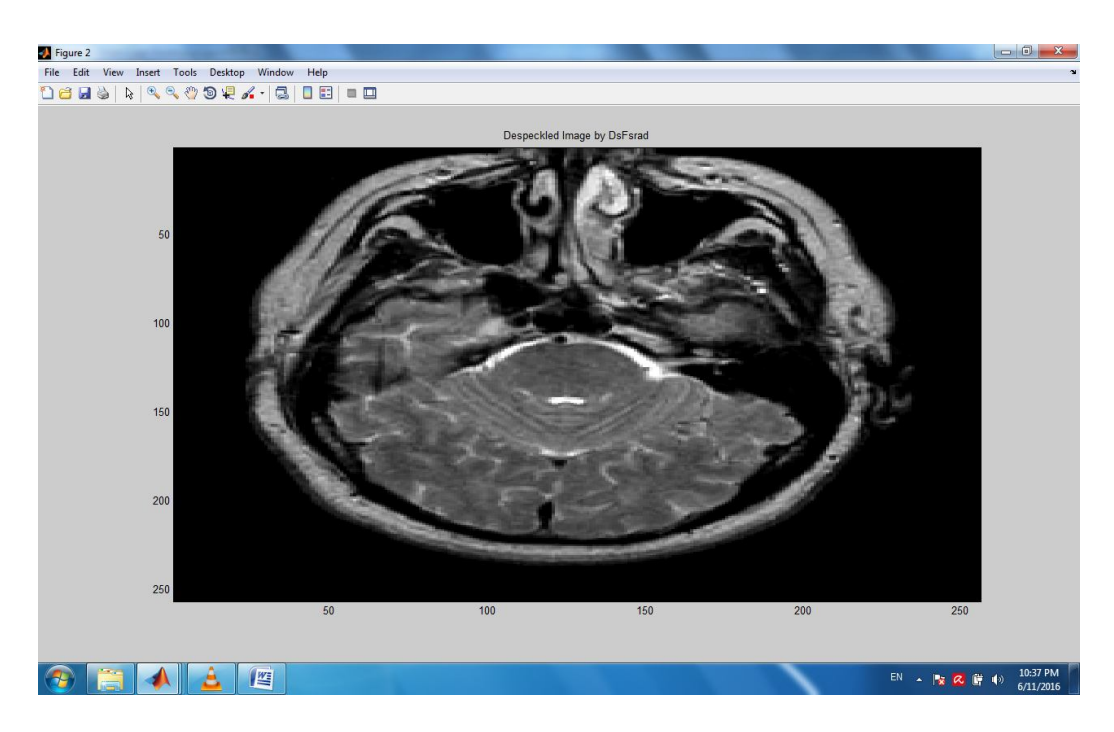


Figure (5.17) brain-hemispheric transaxial II with srad filter

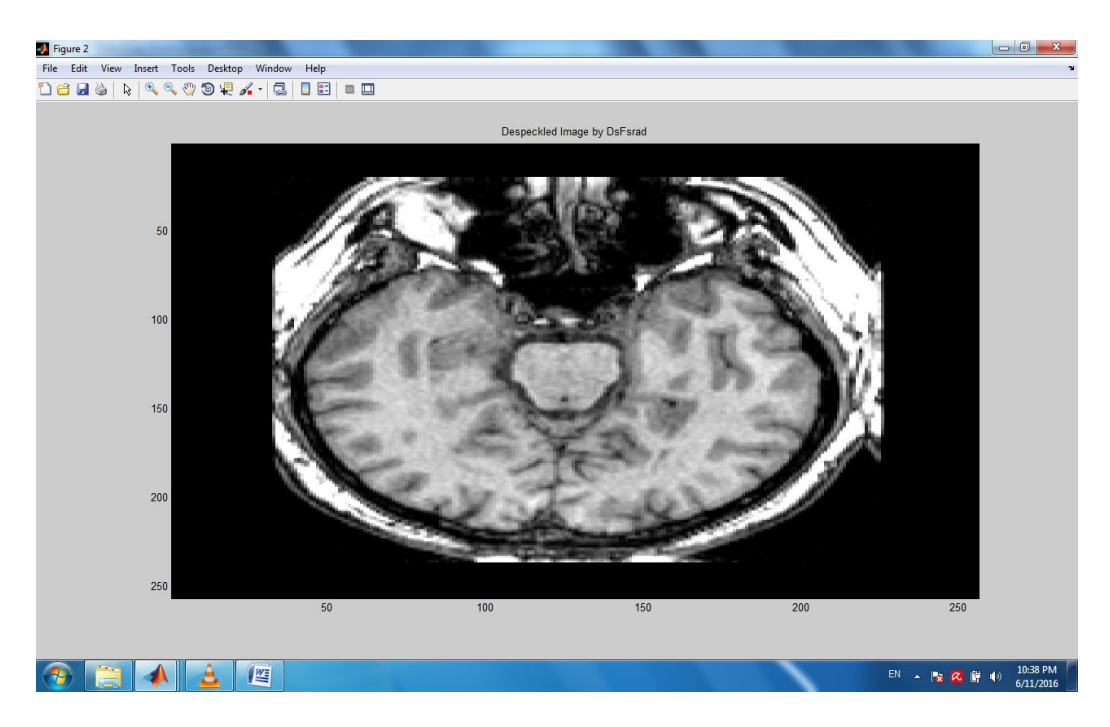


Figure (5.18) brain-hemispheric transaxial II with srad filter



Figure (5.19) brain-hemispheric coronal I with srad filter

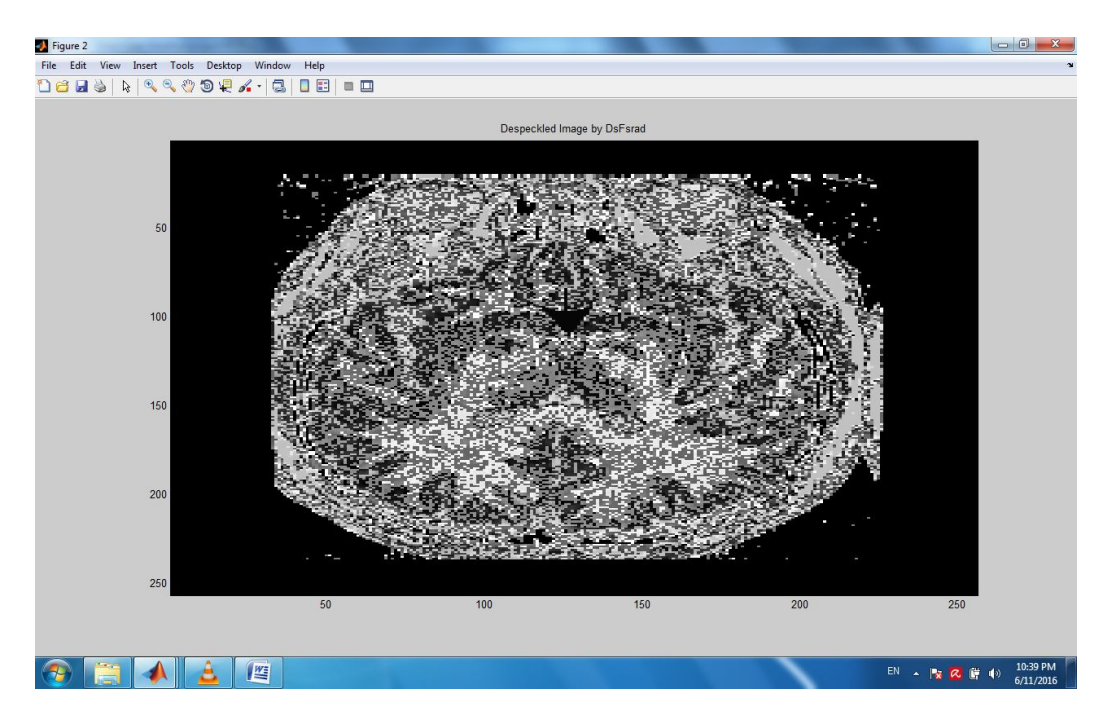


Figure (5.20) brain-hemispheric coronal II with srad filter

5.1.2.4 Bilaterall:

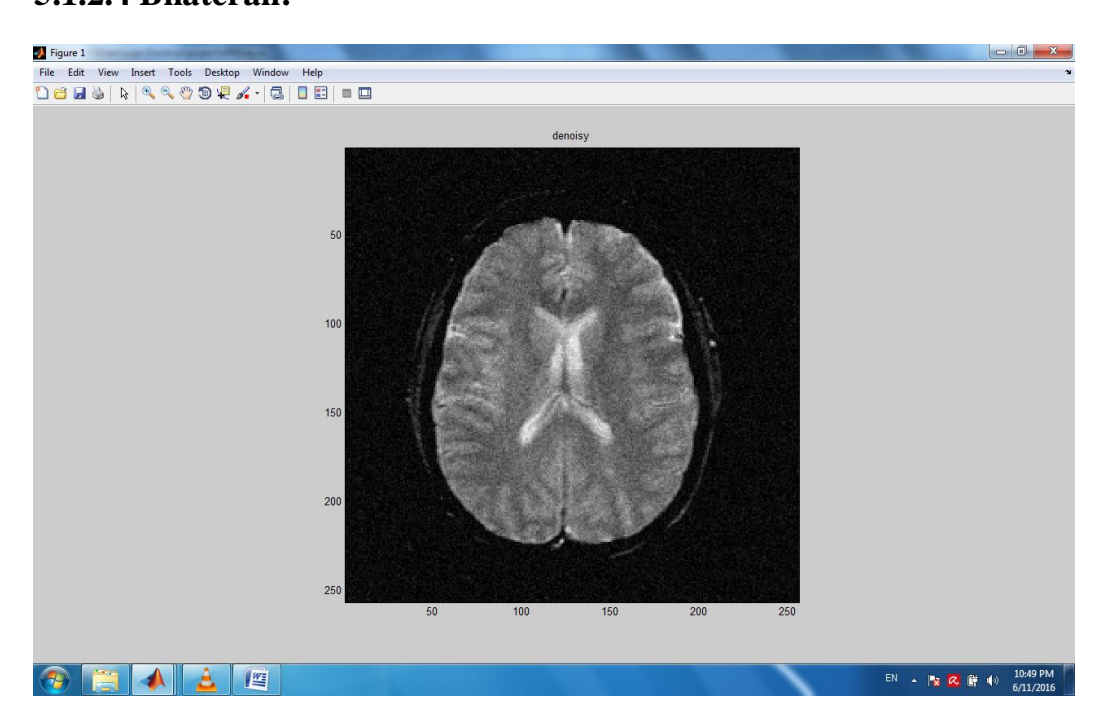


Figure (5.21) show brain-hemispheric transaxial I with Bilaterall filter

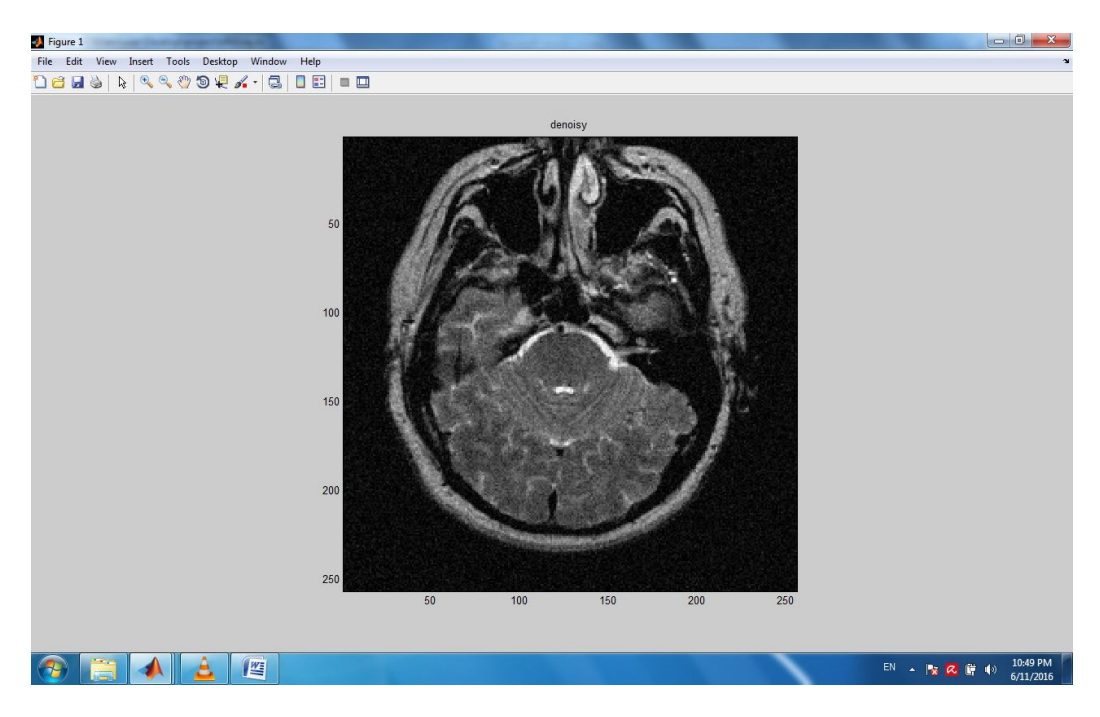


Figure (5.22) show brain-hemispheric transaxial II with Bilaterall filter

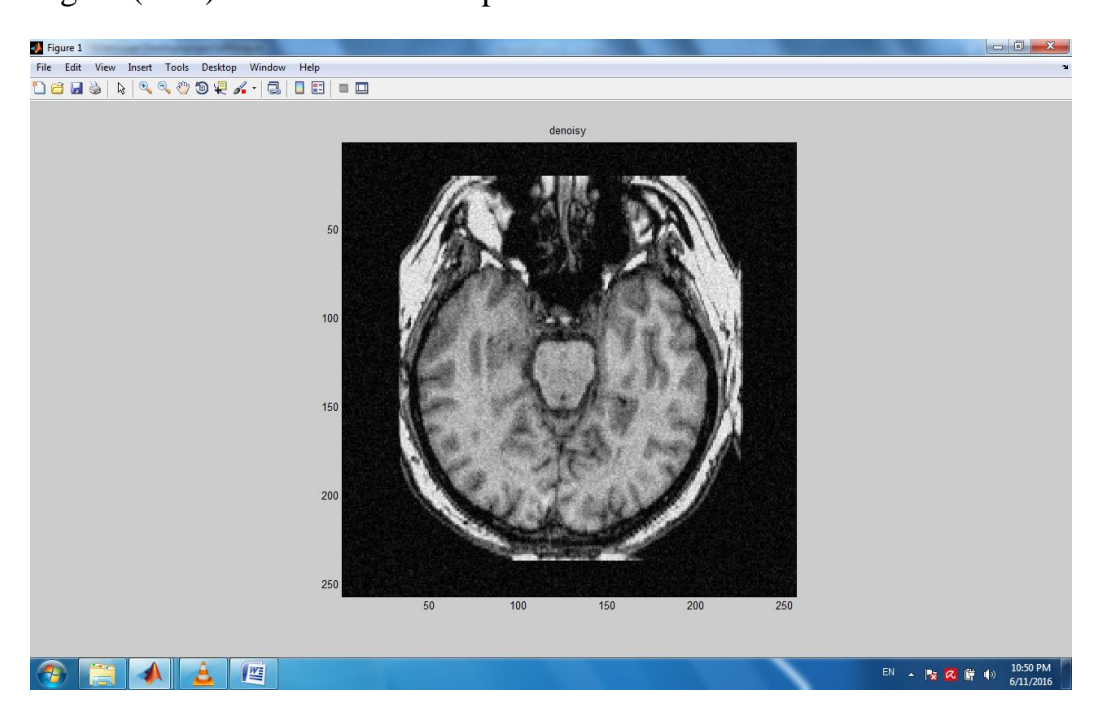


Figure (5.23) show brain-hemispheric transaxial III with Bilaterall filter

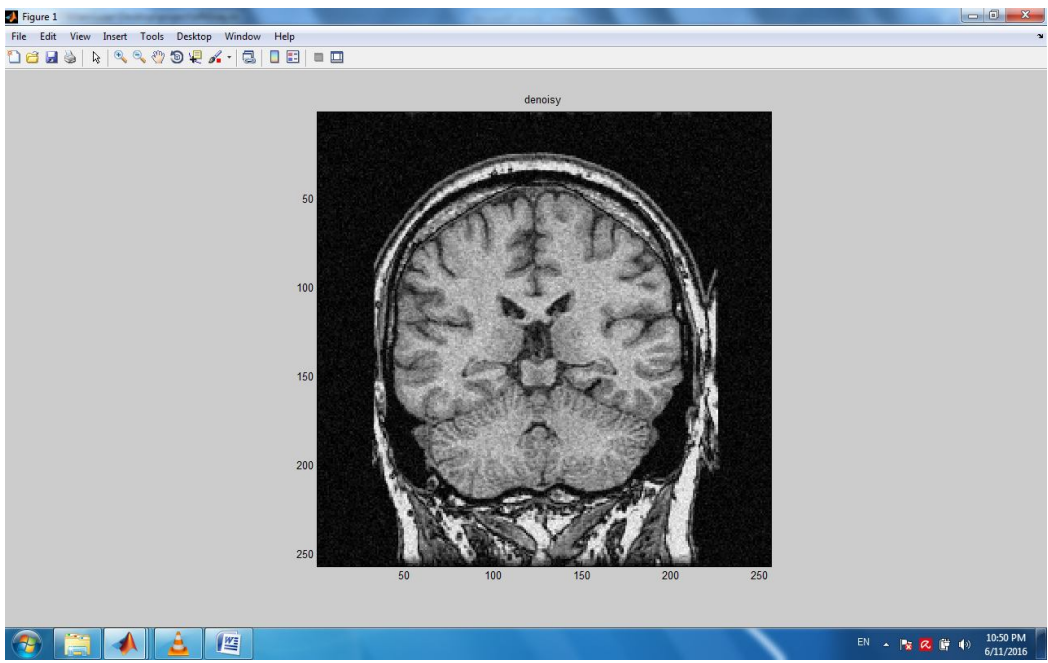


Figure (5.24) show brain–hemispheric coronal I with Bilaterall filter

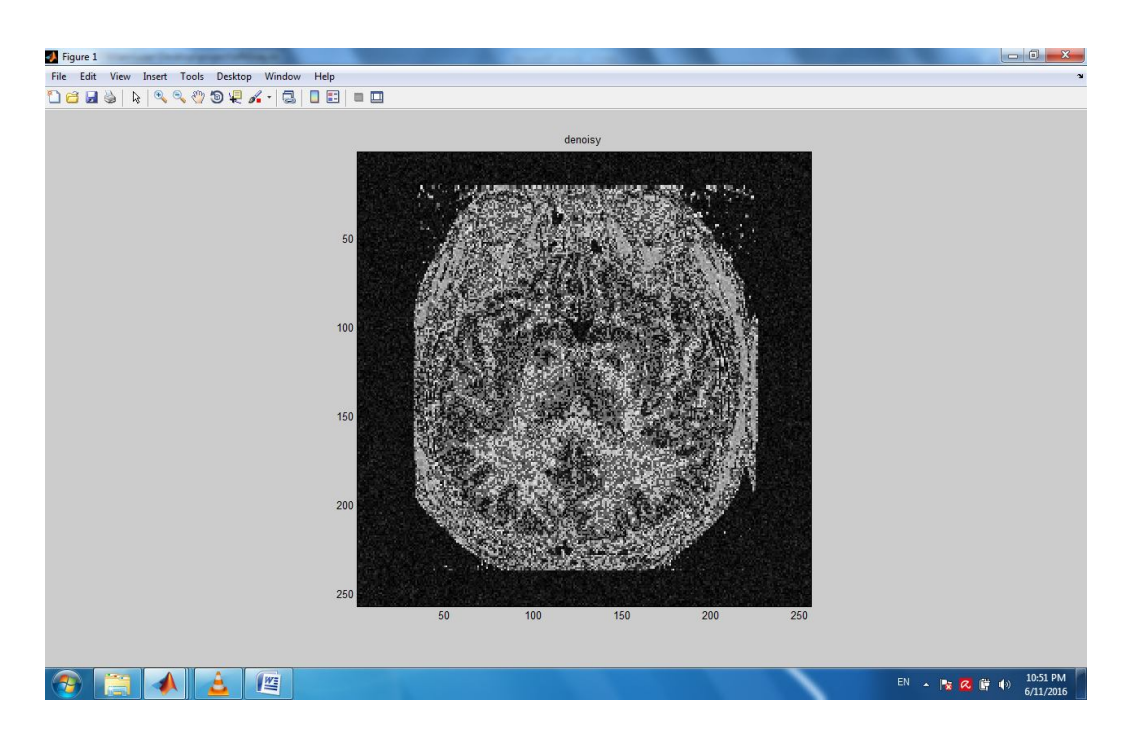


Figure (5.25) show brain-hemispheric coronal II with Bilaterall filter

5.1.2.5 NLmeansfilter:

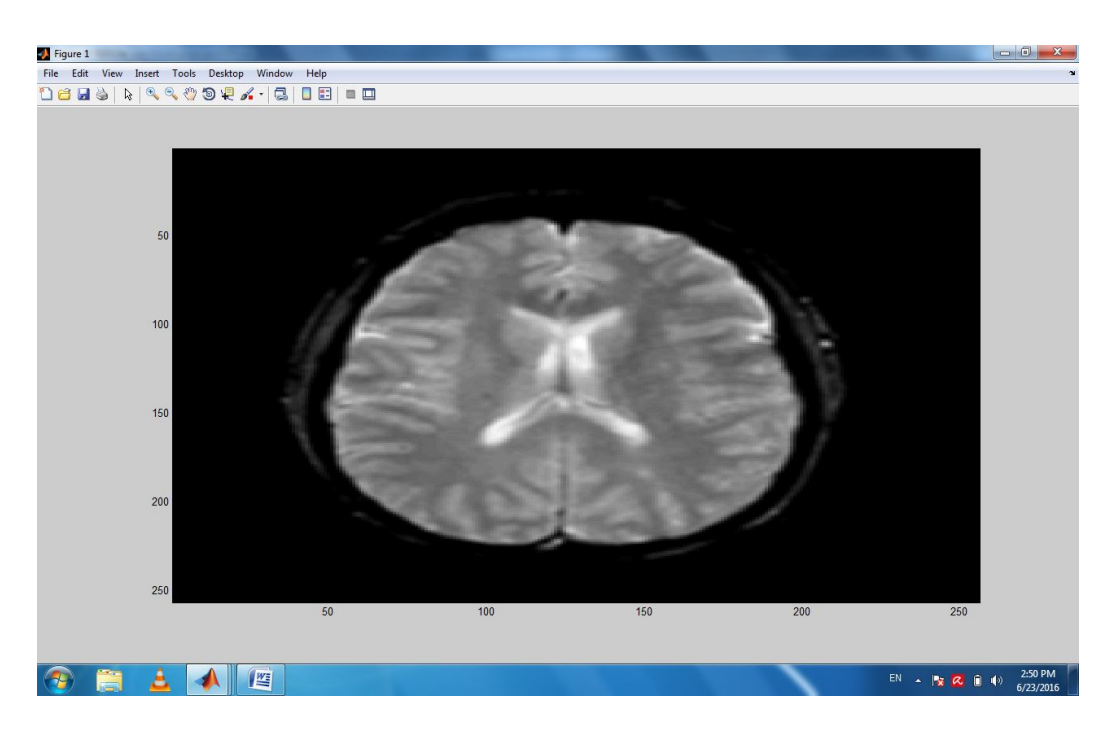


Figure (5.26) show brain–hemispheric transaxial I with NLmeansfilter filter

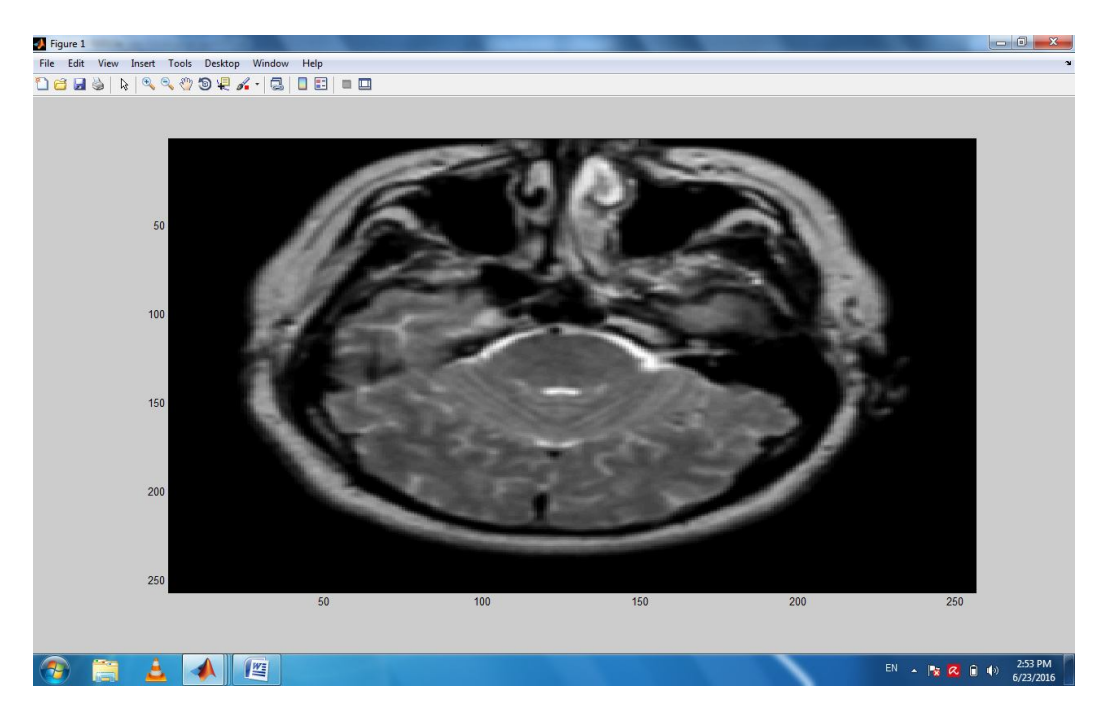


Figure (5.27) show brain-hemispheric transaxial II with NLmeansfilter filter

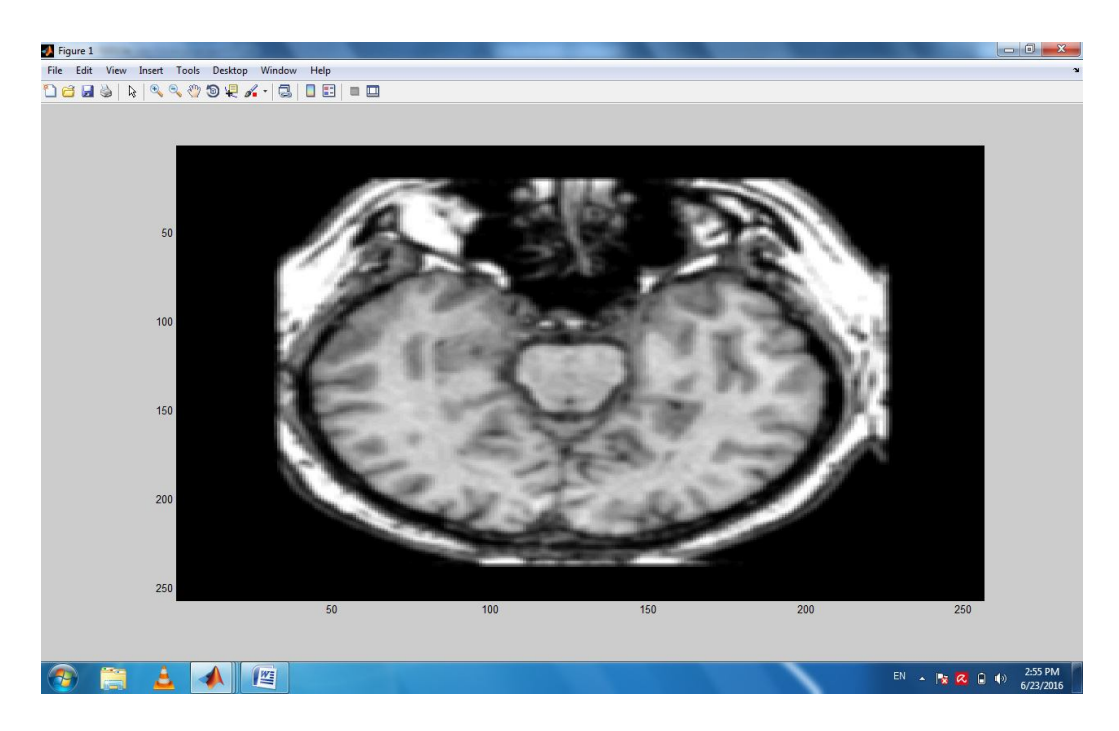


Figure (5.28) show brain–hemispheric transaxial III with NLmeansfilter filter



Figure (5.29) show brain–hemispheric coronal I with NLmeansfilter filter

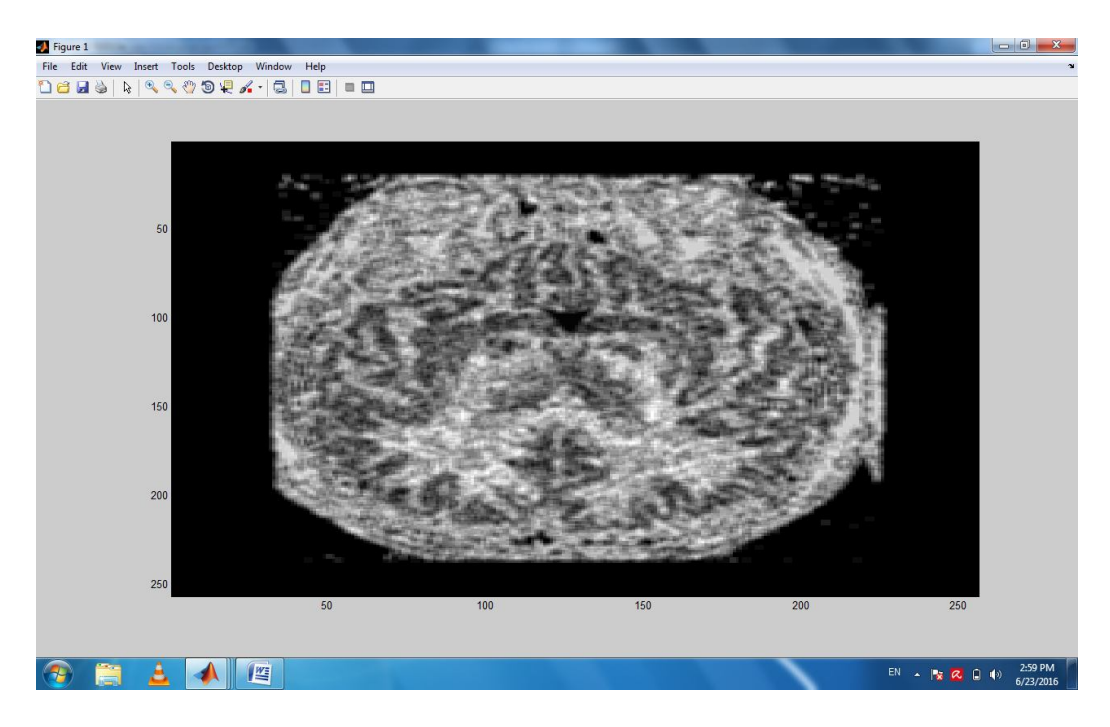


Figure (5.30) show brain-hemispheric coronal II with NLmeansfilter filter

5.1.2.6 hybrid median with wavelet(in low-low):

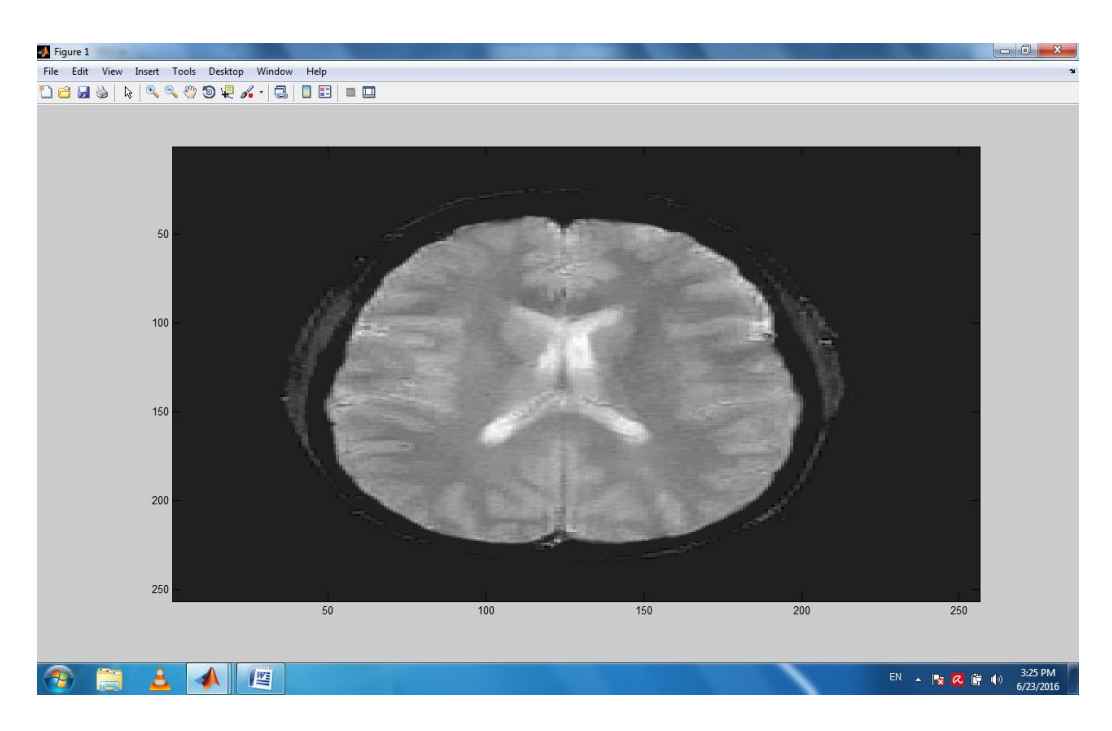


Figure (5.31) show brain–hemispheric transaxial I by hybrid median with wavelet(in low-low)

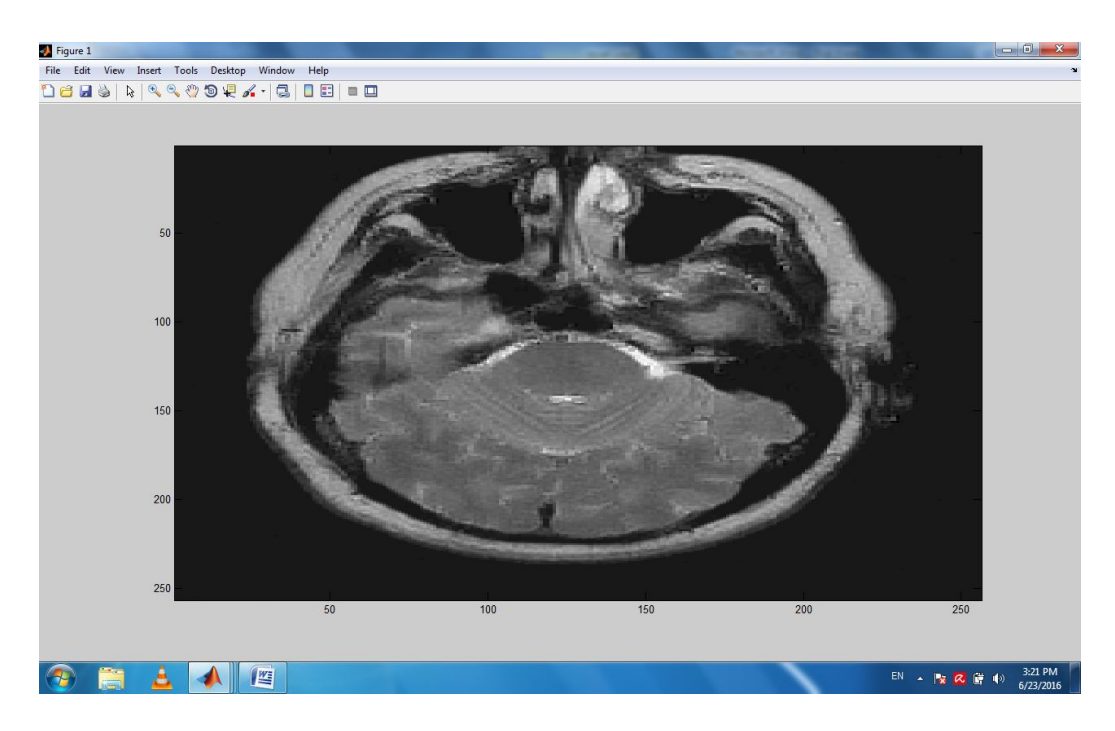


Figure (5.32) show brain–hemispheric transaxial II by hybrid median with wavelet(in low-low)

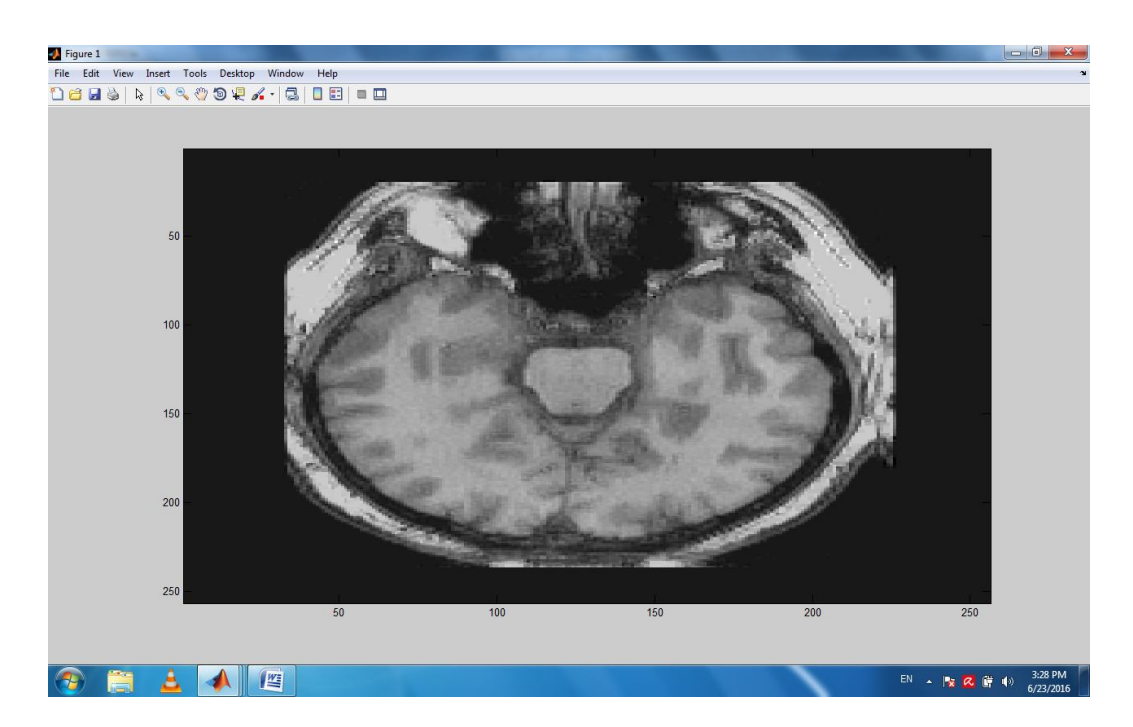


Figure (5.33) show brain–hemispheric transaxial III by hybrid median with wavelet(in low-low)

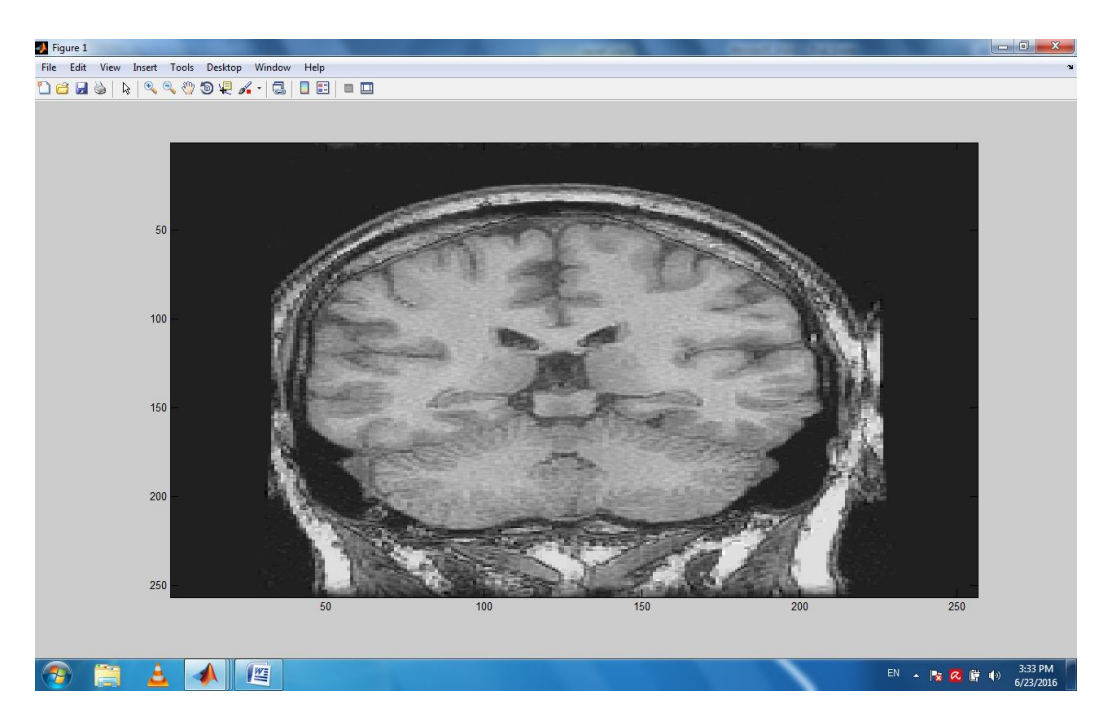


Figure (5.34) show brain–hemispheric coronal I by hybrid median with wavelet(in low-low)

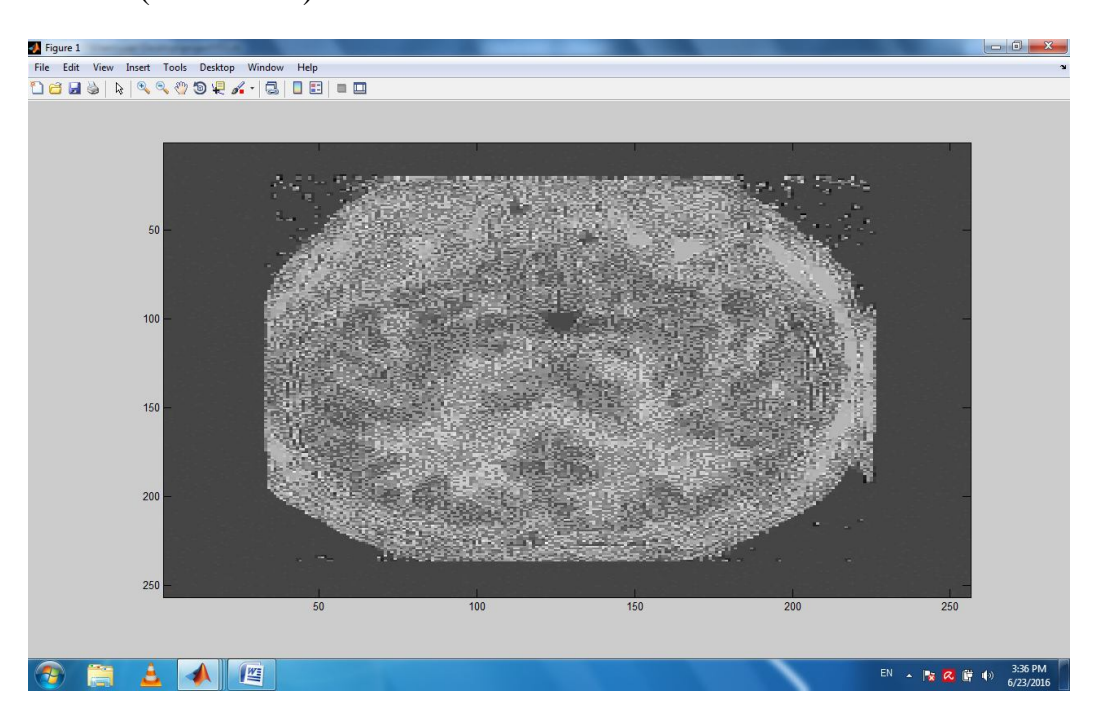


Figure (5.35) show brain–hemispheric coronal II by hybrid median with wavelet(in low-low)

5.1.3.hybrid median with wavelet:

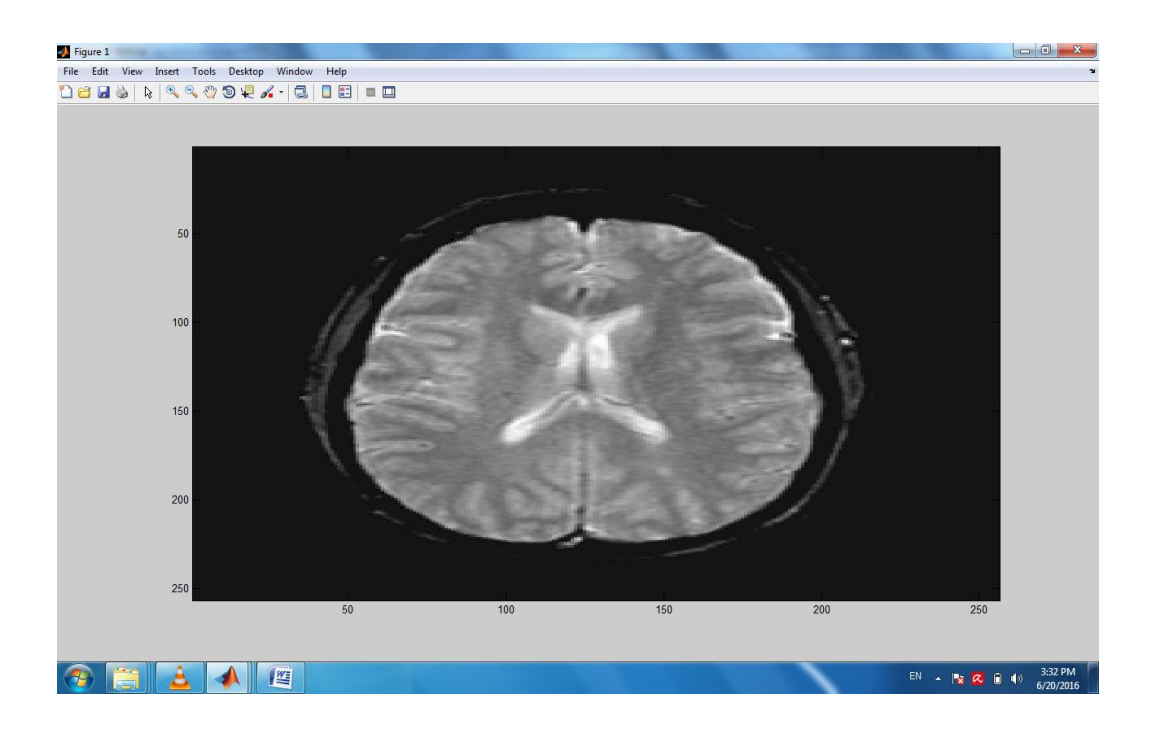


Figure (5.36) show brain—hemispheric transaxial I with hybrid median filter+ wavelet

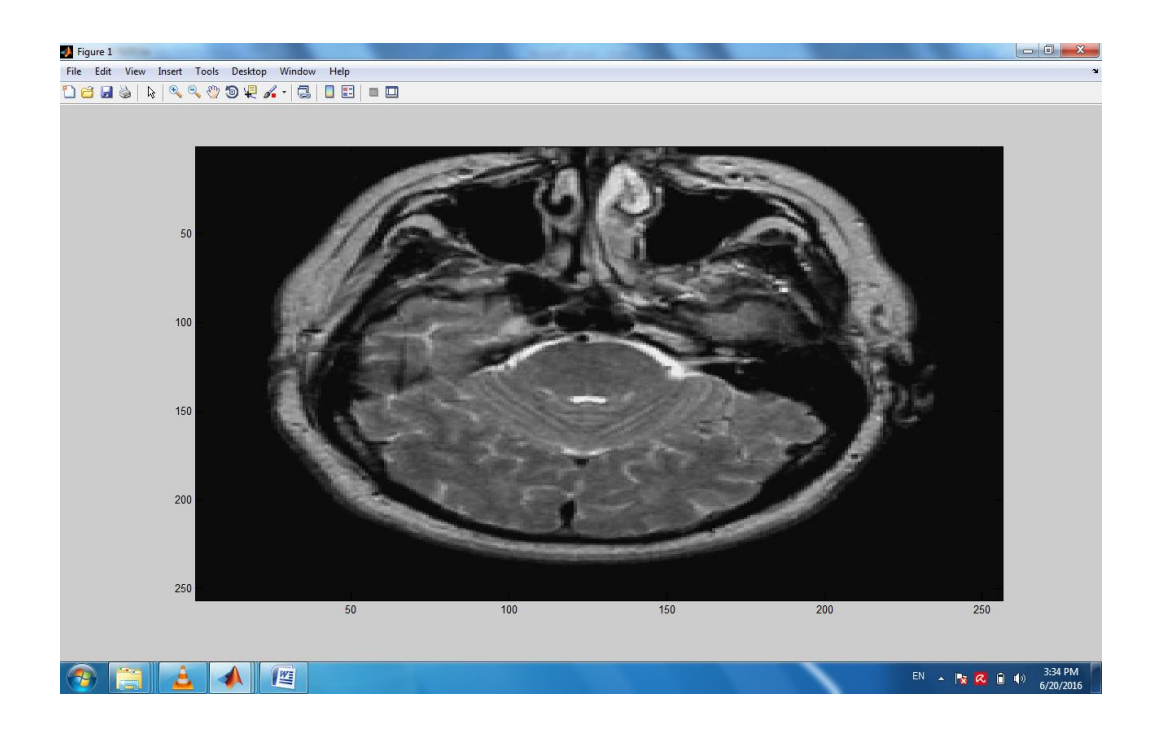


Figure (5.37) show brain–hemispheric transaxial II with hybrid median filter+ wavelet

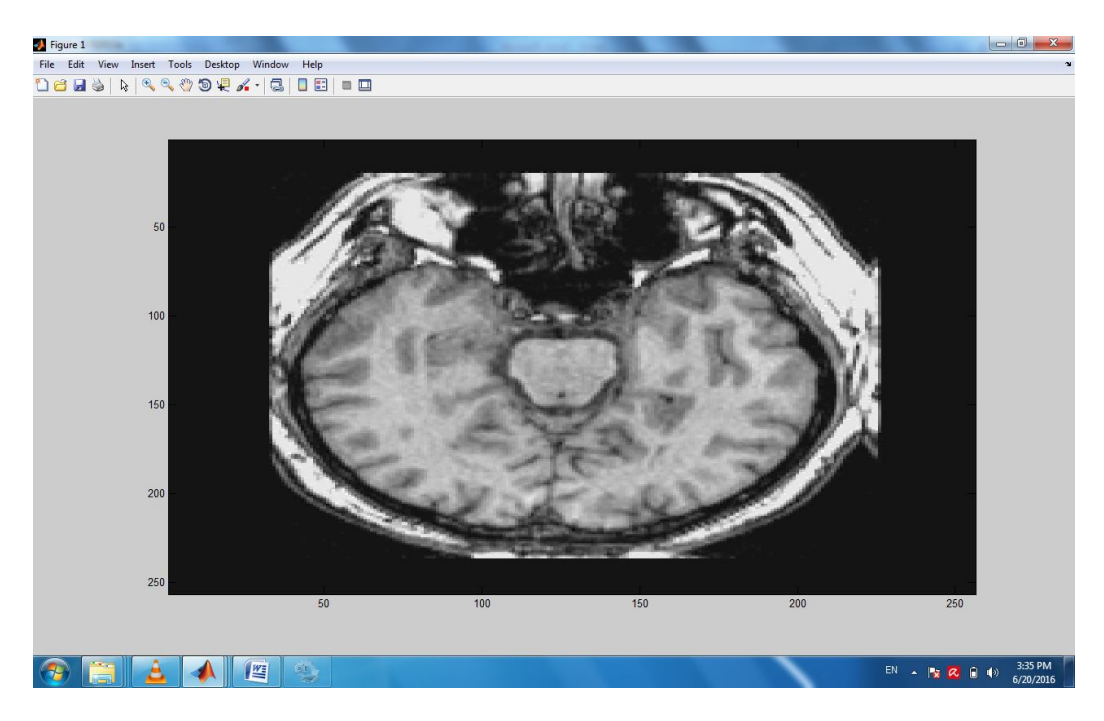


Figure (5.38) show brain—hemispheric transaxial III with hybrid median filter+ wavelet



Figure (5.39) show brain–hemispheric coronal I with hybrid median filter+ wavelet

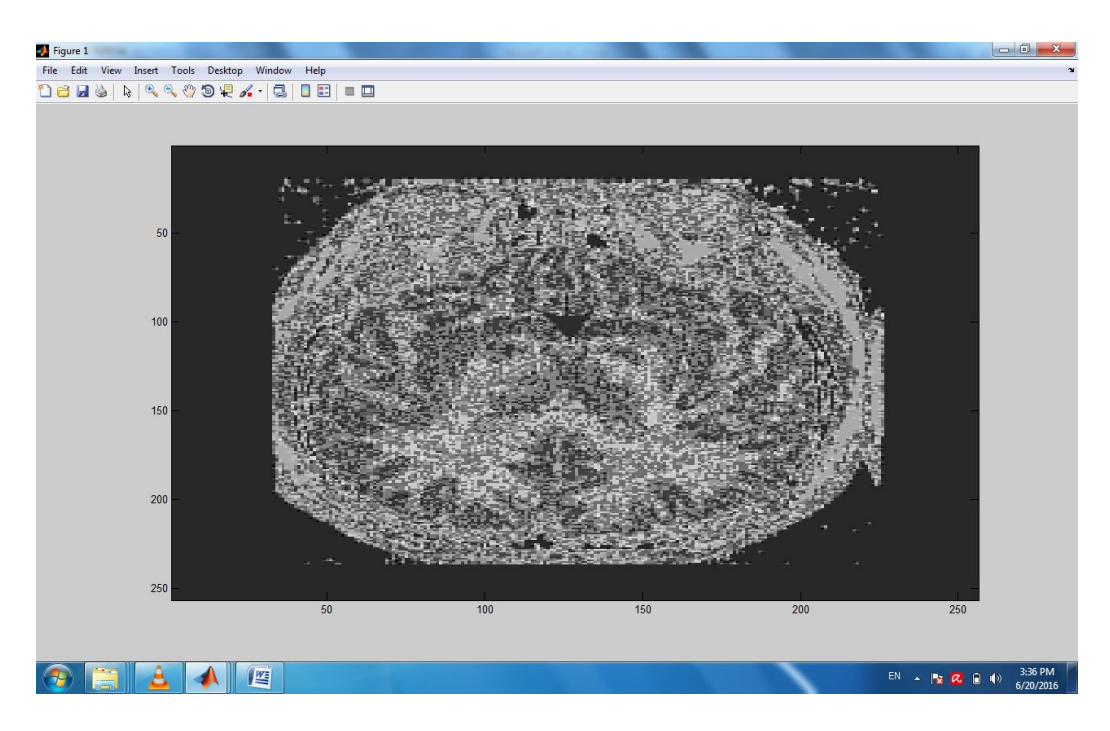


Figure (5.40) show brain-hemispheric coronal II with hybrid median filter+ wavelet

Table(5.1) show the comparative resulted of filter using MES RMES PNSR SNR with the same images .

Images	FILTER	MES	RMES	PSNR	SNR
brain-	hybrid	15.1203	3.8885	36.3692	83.6696
hemispheric	median				
transaxial I					
brain-	srad	6.0863E+03	78.0149	10.3213	23.6874
hemispheric					
transaxial I					
brain-	tvdenoise	207.0762	14.3901	25.0035	59.5395
hemispheric					
transaxial I					
brain-	bilateral	231.8027	15.2251	24.5136	58.3085
hemispheric					
transaxial I					
brain-	NLmeansfilter	24.5530	4.9551	34.2638	78.8275
hemispheric					
transaxial I					
brain-	hybrid	37.9404	6.1596	32.3738	74.4651
hemispheric	median in				
transaxial I	low-low sub-				
	band				

brain-	hybrid	48.8090	6.9863	31.2798	71.9476
hemispheric	median				
transaxial II					
brain-	srad	5.1997e+03	72.1087	11.0050	25.2618
hemispheric	0.44	0117770100	,		20.20.0
transaxial II					
brain-	tvdenoise	189.4590	13.7644	25.3896	60.0927
hemispheric	· · · · · · · · · · · · · · · · · · ·	107.1070	10.7011	20.0070	00.0727
transaxial II					
brain-	bilateral	211.4540	14.5415	24.9126	59.9167
hemispheric	Dilatoral	211.1010	11.0110	21.7120	07.7107
transaxial II					
brain-	NLmeansfilter	73.2183	8.5568	29.5186	67.9000
hemispheric	Nemeansine	73.2103	0.5500	27.3100	07.7000
transaxial II					
brain-	hybrid	117.2592	10.8286	27.4733	63.5495
hemispheric	median in	117.2372	10.0200	21.4133	03.5495
transaxial II	low-low sub-				
панзаланн	band				
	Dariu				
brain-	hybrid	81.6286	9.0349	29.0464	66.8081
	median	01.0200	9.0349	29.0404	00.0001
hemispheric transaxial III	median				
	2024	1 2127 - 04	114 5740	/ 0021	1/ 0000
brain-	srad	1.3127e+04	114.5743	6.9831	16.0008
hemispheric					
transaxial III	tudonoi o o	107 2212	12 (022	25 4410	/1 /007
brain-	tvdenoise	187.2312	13.6832	25.4410	61.4097
hemispheric					
transaxial III	19.1	010 / 10 1	14.5107	0.4.0000	(0.507.4
brain-	bilateral	210.6434	14.5136	24.9293	60.5074
hemispheric					
transaxial III	All City	4/7/070	10.0475	05.0044	50 (40)
brain-	NLmeansfilter	167.6370	12.9475	25.9211	59.6196
hemispheric					
transaxial III					
brain-	hybrid	177.0425	13.3057	25.6840	64.3512
hemispheric	median in				
transaxial III	low-low sub-				
	band				
brain-	hybrid	165.1362	12.8505	25.9864	59.7618
hemispheric	median				
coronal I					
brain-	srad	1.3742E+04	117.2254	6.7844	15.5433 1
hemispheric					
coronal I					
brain-	tvdenoise	182.2653	13.5006	25.5578	61.4601
hemispheric					
coronal I					
brain–	bilateral	202.5255	14.2311	25.1000	60.5328

hemispheric coronal I					
brain- hemispheric coronal I	NLmeansfilter	297.4014	17.2453	23.4314	53.8882
brain- hemispheric coronal I	hybrid median in low-low sub- band	252.8244	15.9005	24.1366	58.9969
brain- hemispheric coronal II	hybrid median	557.8386	23.6186	20.6997	37.2383
brain- hemispheric coronal II	srad	4.3116E+03	65.6628	11.8184	16.7870
brain– hemispheric coronal II	tvdenoise	196.6553	14.0234	25.2277	52.0213
brain– hemispheric coronal II	bilateral	208.0289	14.4232	24.9836	52.0982
brain– hemispheric coronal II	NLmeansfilter	845.0563	29.0699	18.8959	33.1017
brain– hemispheric coronal II	hybrid median in low-low sub- band	192.6686	13.8805	25.3167	52.7964

Table (5.2) show the comparative resulted of hybrid median filter after using the wavelet by MES RMES PNSR SNR.

Images	MES	RMES	PSNR	SNR
brain- hemispheric	1.9434	1.3933	45.2840	97.7607
transaxial I				
brain- hemispheric transaxial II	5.3083	2.3040	40.9153	95.8781
brain- hemispheric transaxial III	13.8581	3.7226	36.7478	86.7914
brain- hemispheric coronal I	24.0048	4.8995	34.3618	81.3720
brain– hemispheric coronal II	149.1810	12.2140	26.4277	54.9220

5.2 Discussions:

In this research, experiments are conducted on five different MRI medical images. The noise type is Rician noise level $\sigma = .05$. the filters (hybrid median, srad, tvdenoise, bilaterall, NLmeansfilter) apply on the noisy images . and from table one we observed that; the hybrid median have a high (SNR, PSNR) and low (MSE, RMES). Haar wavelet transforms are applied for de-noising; Different PSNR MSE, SNR and RMES values are calculated on each image. It is clear from the table one; that using wavelet to decomposition image before filtering and filtering using hybrid median is better than using hybrid median directed for the purpose of de-noising in the MRI medical images. De-noising is performed at Rician noise σ =.05, on MRI images by using Haar wavelet with hybrid median filter in high-high sub-band is the best result (the values of SNR ,PSNR are increase while MSE and RMES are decrease)from using hybrid median on all images except on image 5 we observed that, apply hybrid median in low-low sub-band is best result that refer to ; hybrid median is smoothing filter and it effect on the edges and the LL is contents the main feature of image more filtration of LL (or image in general) may lead to blurring image and decreasing the quality of image (as general) but in brain-hemispheric coronal II image it is very noisily image and more smoothing enhance it.

Chapter six Conclusion & recommendation

6.1 Conclusion:

According to the test carried throughout this study ,it can be concluded that:

The rician noise is a major type of noise embedded with MRI image. Applying the filter it can be reducing the noise by high ratio of SNR &PSNR while low ratio of MSE & RMES and this ratios different from filter to other and from image to other depended on the feature and histogram of image .apply the wavelet technique it enhancement the results in all filters . the low-low sub-band contain the details of image and more filtration can be lead to blurring image while the high-high sub-band contain the noise and more filtration lead to enhancement results . The hybrid median give us the best result that means the hybrid median is effective rician noise .

6.2 Recommendation:

recommend to apply more types of wavelet to get more good resolution , high degree of filtration images and high level from SNR ,PSNR .

Or apply any transformation technique like (Contourlet or Sanlet) to get best result.

References:

- [1] Performance Evaluation of Various Denoising Filters for Medical Image, P.Deepal and M.Suganthi, Department of Computer Science and Engineering Muthayammal Engineering College, Rasipuram. 2 Department of Electronics and Engineering, Mahendra College of Engineering, Salem, P.Deepa et al, / (IJCSIT) International Journal of Computer Science and Information Technologies, (2014).
- [2] Contrast Enhancement of brain MRI images using histogram based techniques, Pratik Vinayak Oak1, Prof.Mrs.R.S.Kamathe2 ME (Signal Processing), PES's Modern College of Engineering, Pune1 Assistant Professor, E &TC Dept. PES's Modern College of Engineering, Pune, International Journal Of Innovative Research In Electrical, Electronics, Instrumentation And Control Engineering Vol. 1, Issue (3, June 2013).
- [3] Image De-noising using Median Filter and DWT Adaptive Wavelet Threshold, Ms.Dhanushree.V1, Mr.M.G.srinivasa2 1(PG Scholar (ECE), maharaja institute of Technology Mysore, India) 2(Asst.professor (ECE), maharaja institute of Technology Mysore, India)
- [4] Digital Image Processing, R. Gonzalez and R. Woods, 2nd edn., Prentice-Hall, New York (2002).
- [5] Fundamentals of Image Processing, Ian T. Young, Jan J. Gerbrands ,Lucas J. van Vliet Delft University of Technology
- [6] Region Growing Adaptive Contrast Enhancement Of Medical MRI Images, Sonia Goyal* and Seema Baghla Department of Computer Science and Engineering, YCOE College of Engineering, Talwandi Sabo,India, Journal of Global Research in Computer Science Volume 2, No. 7, (July 2011).
- [7] Contrast Enhancement of MRI Images A Review, Rajulath Banu A.K1., Dr. A. Ranjith Ram2 1, 2Department of ECE, Government College of Engineering Kannur, Kannur, Kerala 670 563, India, International Journal of Emerging Technology and Advanced Engineering,

Volume 5, Issue (6, June 2015).

- [8] Medical Images Edge Detection Based on Mathematical Morphology, Prof. J.Mehena Department of Electronics & Telecommunication Engg. DRIEMS, Tangi, Cuttack.
- [9] Magnetic Resonance Imaging (MRI), http://www.slideworld.org/.
- [10] Introduction to Magnetic Resonance Imaging Techniques, Lars G. Hanson, larsh@drcmr.dk Danish Research Centre for Magnetic Resonance (DRCMR), Copenhagen University Hospital Hvidovre Latest document version.
- [11] Total Variation Filtering, Ivan W. Selesnick and _Ilker Bayram ,(February, 2010).
- [12]http://homepages.inf.ed.ac.uk/rbf/CVonline/LOCAL_COPIES/MAN DUCHI1/Bilateral_Filtering.html
- [13]http://homepages.inf.ed.ac.uk/rbf/CVonline/LOCAL_COPIES/VELD HUIZEN/node18.html
- [14] Image Enhancement using Histogram Equalization and Spatial Filtering, Fari Muhammad Abubakar1 ,Department of Electronics Engineering ,Tianjin University of Technology and Education (TUTE) ,Tianjin, P.R. China
- [15] The Rician Distribution of Noisy MRI Data, Magn Reson Med. Author manuscript; available in PMC (25, February, 2008).
- [16] Effectiveness of Contourlet vs Wavelet Transform on Medical Image Compression: a Comparative Study, Negar Riazifar, and Mehran Yazdi, International Journal of Electrical, Computer, Energetic, Electronic and Communication Engineering.

.

[17] Medical Image Denoising In The Wavelet Domain Using Haar And DB3 Filtering, anwaljot Singh Sidhu1, Baljeet Singh Khaira2, Ishpreet Singh Virk3, International Refereed Journal of Engineering and Science (IRJES) ISSN (Online) 2319-183X, (Print) 2319-1821 Volume 1, Issue 1 (September 2012), PP.001-008.

- [18] A Review Paper: Noise Models In Digital Image Processing, Ajay Kumar Boyat1 and Brijendra Kumar Joshi2, Signal & Image Processing: An International Journal (SIPIJ) Vol.6, No.2, (April 2015).
- [19] https://en.wikipedia.org/wiki/Root-mean-square_deviation.

.

[20] An Adaptive Image Enhancement Technique Preserving Brightness Level Using Gamma Correction, Ankit Aggarwal, R.S. Chauhan and Kamaljeet Kaur ISSN 2231-1297, Volume 3, Number 9 (2013), pp. 1097-1108.